Applied Geochemistry 55 (2015) 62–71

Contents lists available at ScienceDirect

Applied Geochemistry

journal homepage: www.elsevier.com/locate/apgeochem

Principles, caveats and improvements in databases for calculating hydrogeochemical reactions in saline waters from 0 to 200 °C and 1 to 1000 atm

C.A.J. Appelo *

Hydrochemical Consultant, Valeriusstraat 11, NL 1071 MB Amsterdam, Netherlands

ARTICLE INFO

Article history:
Available online 13 November 2014

ABSTRACT

Databases distributed with PHREEQC may give widely different results for concentrated solutions. Only the database that uses Pitzer's interaction coefficients provides both correct solubilities and mean activity coefficients. The applicability of this database for predicting scaling by mineral precipitation is extended by fitting interaction coefficients for the Na–K–Mg–Ca–Ba–Cl–CO_2–HCO_3–SO_4–H_4SiO_4 system from isopiestic and solubility data at high temperatures. The pressure dependence of equilibrium constants is calculated from the reaction volume, in which the apparent molar volume of the solutes is derived from density measurements. The apparent volumes are a function of temperature, pressure, and ionic strength, and incorporate complicated changes of the partial molar volumes of the water molecules.

Fugacity coefficients for CO_2 can be obtained reliably with the Peng–Robinson equation of state for gases. The CO_2 ion interaction parameters given by Harvie et al. (1984) for 25 °C are also valid for calculating the CO_2 solubility at high temperatures, pressures and salinities.

PHREEQC input files are available for download, comparing experimental and calculated solubilities of (Na, K, Mg, Ca, Ba) minerals of chlorides, sulfates and carbonates, and of amorphous silica and CO_2 in concentrated solutions.

1. Introduction

Drilling for oil recovery and CO_2 storage now commonly reaches depths of 4000 m and more, and it is most important to predict the possibility of precipitation by sulfates, carbonates and silicates in the well and its immediate surroundings at the pressures, temperatures, and salinities encountered at those depths. The challenges are to calculate the activity of aqueous solutes at high concentrations, and the change of the equilibrium constants with temperature, and, for the pressure dependence, the change of the aqueous volumes with temperature, pressure and concentration.

Activity coefficients for a dissolved salt are obtained from electrode potentials or from the vapor or osmotic pressure of water, and applying the Gibbs–Duhem relation (Robinson and Stokes, 1959). The volumes of aqueous solutes (needed for calculating the pressure dependence of the equilibria) are found from solution densities (Millero, 1971), and equilibrium constants from the Gibbs energy of the system (heat capacity and entropy) (Atkins and de Paula, 2002). It is easy to check that different databases can give large differences, even for what seems a simple system, *viz* of halite dissolving in water. Fig. 1 shows the mean activity coefficient and the apparent molar volume of NaCl as a function of concentration at 25 °C, and the solubility of halite and the mean activity coefficient at saturation as a function of temperature, comparing values measured and calculated with the databases phreeqc.dat, pitzer.dat and llnl.dat, distributed with PHREEQC (Parkhurst and Appelo, 2013).

Clearly, from Fig. 1, pitzer.dat allows for an accurate calculation of the measured activity coefficients and the halite solubility over the full temperature range of 0–300 °C, but it needs a number of polynomials with five temperature-dependent terms for that. On the other hand, the gradual increase of the halite solubility with temperature can be calculated well with phreeqc.dat, which uses a constant reaction enthalpy for the dissolution reaction (thus, one temperature dependent term) and activity coefficients in solution that decrease according to the Debye-Hückel equation (thus, by the temperature dependence of the dielectric constant of water). However, Fig. 1D shows that these activity coefficients are not correct. Apparently, the error is compensated rather fortuitously when the solubility is calculated. The solubility obtained with llnl.dat is wrong because it includes a solute NaCl complex in the calculations. Finally, Fig. 1B shows that the aqueous molar volume of NaCl increases markedly with concentration, which is

* Tel.: +31 206716366.
E-mail address: appt@hydrochemistry.eu

http://dx.doi.org/10.1016/j.apgeochem.2014.11.007
0883-2927/

calculated accurately by the equations of Appelo et al. (2014), while the formula of Helgeson et al. (1981) gives only acceptable results for concentrations smaller than 2 M NaCl.

For other salts with tabulated mean activity coefficients in Robinson and Stokes (1959), the discrepancies are similar as illustrated for NaCl. It may be possible to adapt the equilibrium constant and calculate a 'correct' solubility, but it is disturbing that the model then can be wrong in a fundamental solution property.

The only correct database in Fig. 1 is the one with Pitzer interaction parameters, developed by Harvie and Weare (1980), Harvie et al. (1984) for calculating solubilities in concentrated solutions at 25 °C, and extended by Plummer et al. (1988) for NaCl in the temperature range from 0 to 300 °C and for some other ions with coefficients in the 0–60 °C range. Pabalan and Pitzer (1987) calculated interaction parameters in the 0–300 °C range from isopiestic measurements of salt solutions and solubilities of simple salts. The set was further extended with other ions, again based on measurements of osmotic coefficients and salt solubilities as done before by e.g. Greenberg and Møller (1989), Marion and Farren (1999), Monnin (1999). The parameters were reoptimized on data used before for pitzer.dat since hard-coded coefficients in the Pitzer equations may be different, or because newer data invalidate the calculated solubility.

The paper gives the basic equations for calculating equilibrium constants, activity coefficients of gases, minerals and solutions, and their temperature dependence. The pressure dependence may be included by adding pressure as a variable in the polynomials (e.g., Pitzer et al., 1984), but it is both more general and more practical for multicomponent geochemical models to use molar volumes for that purpose (Monnin, 1999; Appelo et al., 2014). The factors that influence the variability of the aqueous molar volumes are summarized and illustrated. It is shown that the pressure dependence of the Debye-Hückel equation differs from the one proposed by Pitzer, and that this affects the calculated solubility. Selected figures illustrate the applicability, and the full set that was used for obtaining coefficients or for checking the model is summarized in an appendix together with PHREEQC input files.

2. Principles

The temperature and pressure dependence of the equilibrium constant of reactions is calculated using:

$$d\Delta G_r = -\Delta S_r dT + \Delta V_r dP \tag{1}$$

and

$$d\log K = \frac{-d\Delta G_r}{2.303RT} \tag{2}$$

where ΔG_r is the sum of the Gibbs energy of the products minus the reactants (J/mol), ΔS_r idem for the entropy (J/mol/K), ΔV_r idem for the volume (J/mol/atm), T is temperature (K), P is pressure (atm), R is the gas constant (8.314 J/mol/K), and K is the equilibrium constant (–). The temperature dependence is given by Van't Hoff's equation:

$$\log K_T = \log K_{298} - \frac{\Delta H_r}{2.303R}\left\{\frac{1}{T} - \frac{1}{298}\right\} \tag{3}$$

and the pressure dependence by:

$$\log K_P = \log K_{P=1} - \frac{\Delta V_r}{2.303RT}(P-1) \tag{4}$$

where H is the enthalpy (J/mol).

If the reaction enthalpy varies significantly with temperature, a polynomial is used to calculate the temperature and pressure dependence of $\log K$. If the pressure dependence of solubility is

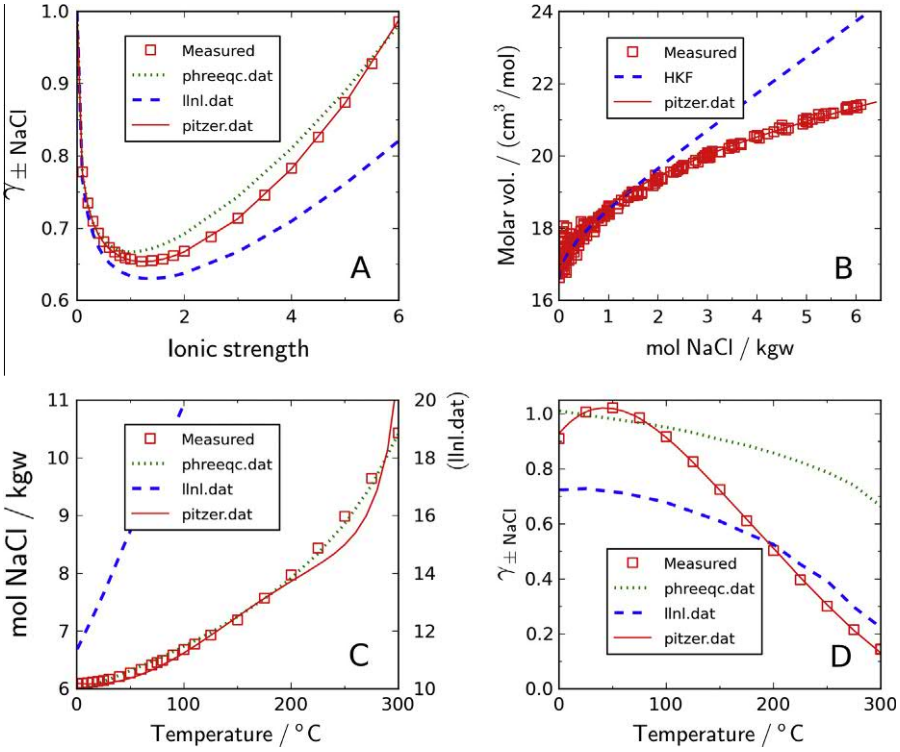

Fig. 1. Comparing measured thermodynamic and physical variables and values calculated with three databases distributed with PHREEQC (phreeqc.dat, llnl.dat, pitzer.dat). (A) Mean activity coefficient of NaCl as a function of concentration at 25 °C (data points from Robinson and Stokes, 1959). (B) Apparent molar volume of NaCl as a function of concentration at 25 °C (data points from Laliberté, 2009, phreeqc.dat and pitzer.dat overlap; dashed line marked as 'HKF' calculated according to Helgeson et al., 1981). (C) Solubility of halite from 0 to 300 °C (data points from Pabalan and Pitzer, 1987, Clarke and Glew, 1985; the solubility calculated with llnl.dat diverges so much that the model line is plotted on a separately defined secondary Y-axis). (D) Mean activity coefficient of NaCl at halite solubility, 0–300 °C (data points from Pitzer et al., 1984).

calculated with a polynomial, changes of aqueous molar volumes with concentration, T and P must be accounted for.

The number of significant digits for the thermodynamic properties is determined by the desired precision in the calculations. Thus, for obtaining the solute activities at equilibrium with a 2-component solid such as halite or calcite within 1.2%, 2 decimals for $\log K$ are sufficient. To calculate $\log K$ over a 100 degree interval from the reference temperature of 298 K, the reaction enthalpy (ΔH_r) must be accurate to 0.23 kJ/mol; and to calculate $\log K$ over a 1000 atm pressure interval requires volumes that are accurate to 0.56 cm^3/mol (at 298 K). The number of digits for the coefficients in a polynomial can be set by the same criterion.

3. Tools

PEST (Doherty, 2003) was used for parameterization of the Pitzer interaction coefficients. PEST uses the Marquardt–Levenberg algorithm for optimizing multiple parameters in a model for a data set. It was developed for interpreting and quantifying geophysical measurements, which usually are poly-interpretable with highly correlated parameters, not unlike the situation in geochemical calculations. Basically, PEST adapts parameters in an input file for a computer model, compares the results from the model output file with data, and minimizes the sum of the squared differences. It provides standard deviations and correlation coefficients for the parameter values and other statistic properties of the model that are helpful for removing redundant parameters and retaining only significant digits in the numbers.

Old data were digitized from tables using KADMOS (reRecognition GmbH) for IrfanView, and from figures with WinDig Data digitizer. Molar volumes of aqueous species were obtained from Laliberté (2009).

4. Pressure dependence of reaction constants

The volume change of a reaction can be used to calculate the pressure dependence of a reaction according to Eq. (4). The molar volumes of solids change much less than 0.5 cm^3/mol for the temperature and pressure range considered here, and their (T, P) dependence is neglected. The molar volumes of aqueous solutes, on the other hand, change markedly with T, P and ionic strength (Redlich and Rosenfeld, 1931; Millero, 1971; Helgeson et al., 1981; Appelo et al., 2014). However, for calculating the pressure dependence of solubility, the computer codes SOLMINEQ (Kharaka et al., 1988) and GEMS (Kulik et al., 2012) use only the molar volumes at infinite dilution from the SUPCRT database (Johnson et al., 1992), neglecting the ionic-strength dependence of the aqueous molar volume. Thus, it is important to explain once more how the aqueous molar volumes are determined and what they depend on.

4.1. Partial and apparent aqueous molar volumes

In a binary solution, the apparent molar volume of the solute (cm^3/mol) is defined as (Millero, 1970):

$$V_{m,2} = \frac{V - n_1 V_1^0}{n_2} \text{ at constant } T,\ P, \tag{5}$$

where V is the volume of the solution with n_1 moles of water and n_2 moles of solute, and V_1^0 is the molar volume of pure water.

Apparent molar volumes can be calculated from density measurements:

$$V_m = \frac{1}{m}\left(\frac{1000 + mMW}{\rho} - \frac{1000}{\rho_0}\right) \tag{6}$$

where V_m is the molar volume of the salt (cm^3/mol), m is the molality (mol/kg H_2O), MW is the molecular weight of the salt (g/mol), and ρ and ρ_0 are the densities of the solution and of pure water at the same pressure and temperature, respectively (g/cm^3). The molar volumes obtained with Eq. (6) are *apparent*, because the volume change of the solution is wholly attributed to the solute species, while the molar volume of H_2O is fixed to the value of pure water. In reality, the density change is largely due to the compaction of water molecules by the electrostatic attraction of the water dipoles to the charged ions.

From Eq. (5), the partial molar volume of the solute is

$$V_2 = \left(\frac{\partial V}{\partial n_2}\right)_{P,T,n_1} = V_{m,2} + n_2\left(\frac{\partial V_{m,2}}{\partial n_2}\right)_{P,T,n_1} \tag{7}$$

And, using Gibbs–Duhem, the molar volume of water in a multicomponent solution can be calculated as:

$$V_1 = V_1^0 - \frac{1}{m_{H_2O}}\sum_i \int_0^{m_i} m_i\left(\frac{\partial V_i}{\partial m_i}\right) dm_i. \tag{8}$$

Fig. 2 illustrates the difference between the apparent molar volume of aqueous LiCl, and the partial molar volumes of LiCl and H_2O. The partial molar volume of pure water at 25 °C and 1 atm is 18.07 cm^3/mol. It decreases with increasing concentration of LiCl up to 9.5 M, and then increases to 18.31 cm^3/mol at 20 M LiCl. The partial molar volume of LiCl shows the inverse trend, increasing from 16.6 cm^3/mol at infinite dilution to 21.7 cm^3/mol at 9.5 M,

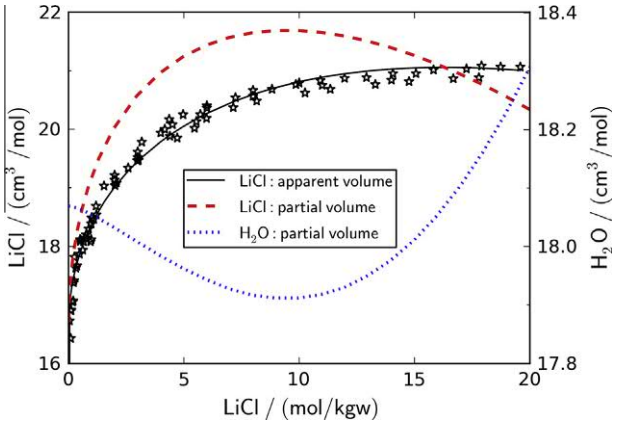

Fig. 2. Partial molar volumes of LiCl and H_2O at 25 °C as a function of the LiCl concentration, calculated from the model for the apparent volume of LiCl. Data points for the apparent volume of LiCl from Laliberté (2009).

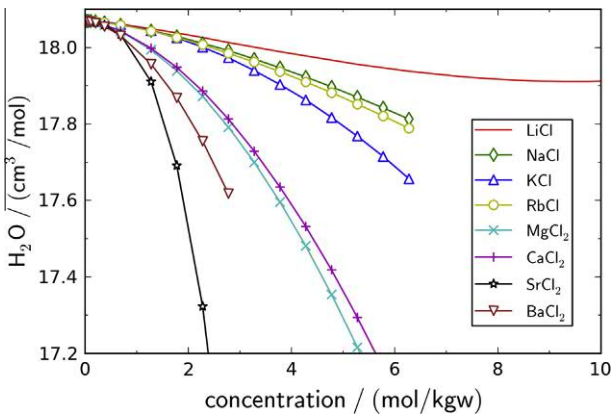

Fig. 3. The partial molar volume of water in solutions of alkali- and alkaline-earth chlorides as a function of the salt concentration.

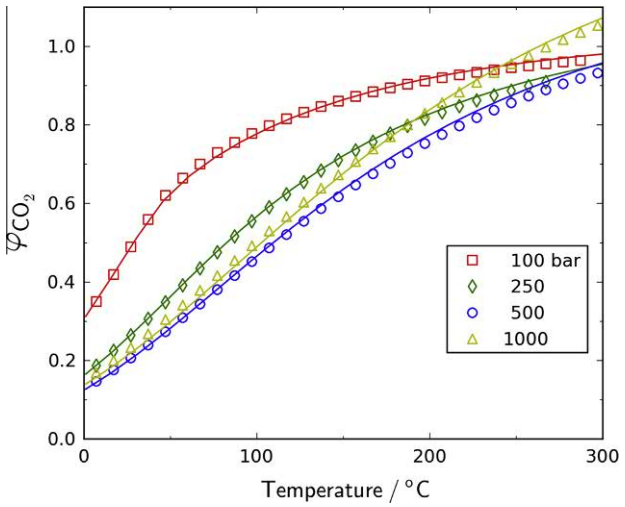

Fig. 4. Fugacity coefficients of CO_2 as a function of temperature and pressure, with model data from Angus et al. (1976) (symbols) and Peng and Robinson (1976) (lines).

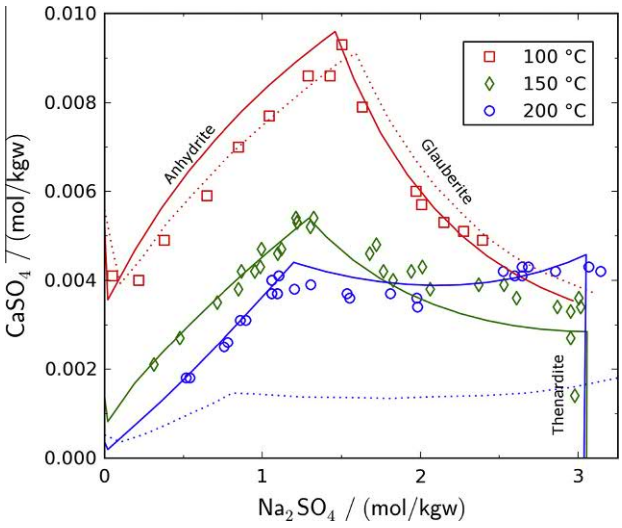

Fig. 6. Solubilities of anhydrite, glauberite and thenardite at 100, 150 and 200 °C. Data points from Freyer and Voigt (2004), with model lines from the Pitzer model presented here, and dotted lines at 100 and 200 °C from the Pitzer model by Greenberg and Møller (1989).

and decreasing then to 20.3 cm^3/mol at 20 M. The apparent and the partial molar volume of LiCl are identical for concentrations <3 μM. Otherwise, the apparent molar volume of LiCl changes less than the partial volume, because it combines the partial volumes of LiCl and of H_2O.

The partial molar volume of water changes differently with concentration in solutions of alkali-chlorides and alkaline-earth chlorides (Fig. 3). Generally, the partial volume decreases with concentration (only for LiCl, densities measured at very high concentrations show that the volume may increase again). The decrease is stronger for alkaline-earths than for alkali ions, which can be attributed to the higher charge of the first. The size of the cation also plays a role, probably because more water molecules can be accommodated around the ion. The trend with ion-size reverts when the O-electron orbit is being occupied, suggesting that chemical binding is a factor as well. The increase of the volume in concentrated LiCl solutions, and the relative increase that starts when the O-orbital is filled, cannot be captured by continuum models, which assume that the dielectric properties of water vary smoothly (Marcus, 2011).

For calculating the pressure dependence, the volume of the solution as a whole must be used, thus including the volumes of both the solutes and water. Helgeson et al. (1981) chose to calculate partial molar volumes, but to obtain the water volumes, this requires cumbersome integrations of the Gibbs–Duhem equation, Eq. (8). More convenient is, to use the apparent, conventional molar volumes, which can be fitted with a polynomial of the form (Appelo et al., 2014):

$$V_{m,i} = V^0_{m,i} + A_v 0.5 z_i^2 \frac{I^{0.5}}{(1+\mathring{a}_i B_\gamma I^{0.5})} + \left(b_{1,i} + \frac{b_{2,i}}{T-228} + b_{3,i}(T-228)\right) I^{b_{4,i}}. \quad (9)$$

where the first term on the right-hand side gives the volume at infinite dilution, the second term is the pressure derivative of the Debye-Hückel equation, and the b parameters in the third term are for fitting the ionic strength dependence. It is puzzling why Johnson et al. (1992) in SUPCRT, developed for the practical application of Helgeson et al.'s (1981) predictive tools, provided only the volumes at zero concentration and not the concentration dependence of the molar volumes, although these were discussed and parameterized by Helgeson et al. (1981).

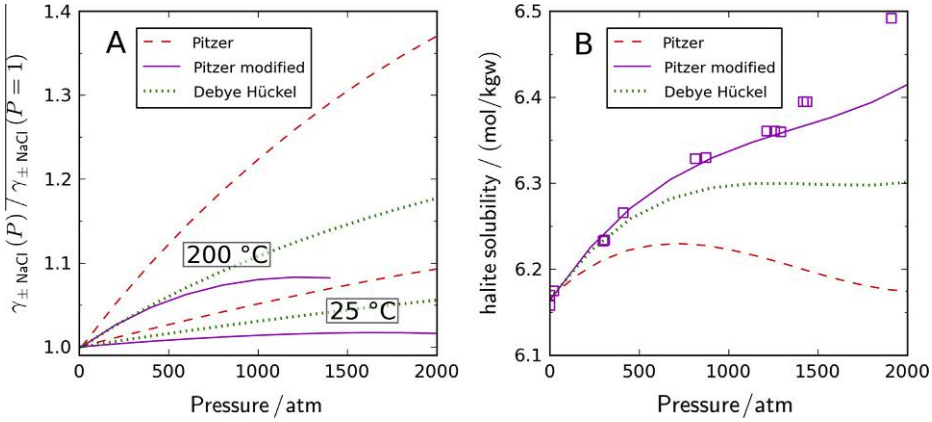

Fig. 5. The relative change of the activity coefficient of aqueous NaCl with pressure at 25 and 200 °C in Pitzer and Debye-Hückel models (A), and the calculated solubility of halite at 25 °C with pressure (B). The dashed lines marked as 'Pitzer' have b = 1.2, the lines marked as 'Pitzer modified' have b = 1.2 – $f(T, P)$, see text. Data points in (B) from Villafáfila García (2005).

Table 1
Data used for obtaining Pitzer solute interaction parameters, and terms for the temperature dependent polynomial of the form: A0 + A1 × (1/*T*–1/T_R) + A2 × ln(*T*/T_R) + A3 × (*T*–T_R) + A4 × (T^2–T_R^2) + A5 × (1/T^2–1/T_R^2), where T_R = 298.15.

Pitzer term, solute species	A0 .. A5	References
−B0		
Ba+2 Cl−	0.5268 0 0 0 0 4.75e4	Blount (1977), Templeton (1960)
Ca+2 Cl−	0.3159 0 0 −3.27e−4 1.4e−7	Holmes et al. (1994), CaCl2 < 5.1 M
Ca+2 HCO3−	0.4	Ellis (1959, 1963), Plummer and Busenberg (1982)
Ca+2 SO4−2	0	Block and Waters (1968), Blount and Dickson (1969), Freyer and Voigt (2004)
Cl− K+	0.04808 −758.48 −4.7062 0.010072 −3.7599e−6	Pabalan and Pitzer (1987)
Cl− Mg+2	0.351 0 0 −9.32e−4 5.94e−7	Pabalan and Pitzer (1987)
Cl− Na+	7.534e−2 9598.4 35.48 −5.8731e−2 1.798e−5 −5e5	Pitzer et al. (1984), Table Al
HCO3− Na+	−0.028	Ellis (1963), Wolf et al. (1989)
K+ SO4−2	3.17e−2 0 0 9.28e−4	Holmes and Mesmer (1986)
Mg+2 SO4−2	0.2135 −951 0 −2.34e−2 2.28e−5	Pabalan and Pitzer (1987)
Na+ SO4−2	2.73e−02 0 −5.8 9.89e−03 0 −1.563e+05	Holmes and Mesmer (1986)
−B1		
Ba+2 Cl−	0.687 0 0 1.417e−2	Blount (1977), Templeton (1960)
Ca+2 Cl−	1.614 0 0 7.63e−3 −8.19e−7	Holmes et al. (1994), CaCl2 < 5.1 M
Ca+2 HCO3−	2.977 0 0 1.22 0 1.43e7	Ellis (1959, 1963), Plummer and Busenberg (1982)
Ca+2 SO4−2	3.546 0 0 5.77e−3	Block and Waters (1968), Blount and Dickson (1969), Freyer and Voigt (2004)
Cl− K+	0.2168 0 −6.895 2.262e−2 −9.293e−6 −1e5	Pabalan and Pitzer (1987)
Cl− Mg+2	1.65 0 0 −1.09e−2 2.60e−5	Pabalan and Pitzer (1987)
Cl− Na+	0.2769 1.377e4 46.8 −6.9512e−2 2e−5 −7.4823e5	Pitzer et al. (1984), Table Al
HCO3− K+	0.25 0 0 1.104e−3	Wolf et al. (1989)
HCO3− Na+	0.415	Ellis (1963), Wolf et al. (1989)
K+ SO4−2	0.756 −1.514e4 −80.3 0.1091	Holmes and Mesmer (1986)
Mg+2 SO4−2	3.367 −5.78e03 0 −1.48e−1 1.576e−4	Pabalan and Pitzer (1987)
Na+ SO4−2	0.956 2.663e3 0 1.158e−2 0 −3.194e5	Holmes and Mesmer (1986)
−B2		
Ca+2 Cl−	−1.13 0 0 −0.0476	Holmes et al. (1994), CaCl2 < 5.1 M
Ca+2 SO4−2	−59.3 0 0 −0.443 −3.96e−6	Block and Waters (1968), Blount and Dickson (1969), Freyer and Voigt (2004)
HCO3− Na+	0 0 0 −0.11	Ellis (1963), Wolf et al. (1989)
Mg+2 SO4−2	−32.45 0 −3.236e3 21.812 −1.8859e−2	Pabalan and Pitzer (1987)
−C0		
Ba+2 Cl−	−0.143 −114.5	Blount (1977), Templeton (1960)
Ca+2 Cl−	1.4e−4 −57 −0.098 −7.83e−4 7.18e−7	Holmes et al. (1994), CaCl2 < 5.1 M
Ca+2 SO4−2	0.114	Block and Waters (1968), Blount and Dickson (1969), Freyer and Voigt (2004)
Cl− K+	−7.88e−4 91.27 0.58643 −1.298e−3 4.9567e−7	Pabalan and Pitzer (1987)
Cl− Mg+2	0.00651 0 0 −2.50e−4 2.418e−7	Pabalan and Pitzer (1987)
Cl− Na+	1.48e−3 −120.5 −0.2081 0 1.166e−7 11121	Pitzer et al. (1984), Table Al
HCO3− Na+	0	Ellis (1963), Wolf et al. (1989)
K+ SO4−2	8.18e−3 −625 −3.30 4.06e−3	Holmes and Mesmer (1986)
Mg+2 SO4−2	2.875e−2 0 −2.084 1.1428e−2 −8.228e−6	Pabalan and Pitzer (1987)
Na+ SO4−2	3.418e−3 −384 0 −8.451e−4 0 5.177e4	Holmes and Mesmer (1986)
−PSI		
Ca+2 Cl− Na+	−1.48e−2 0 0 −5.2e−6	Block and Waters (1968), Blount and Dickson (1969), Freyer and Voigt (2004)
Ca+2 Cl− SO4−2	−0.122 0 0 −1.21e−3	Block and Waters (1968), Blount and Dickson (1969), Freyer and Voigt (2004)
Ca+2 Na+ SO4−2	−0.055 17.2	Block and Waters (1968), Blount and Dickson (1969), Freyer and Voigt (2004)
Cl− Na+ SO4−2	0	Block and Waters (1968), Blount and Dickson (1969), Freyer and Voigt (2004)
Ca+2 K+ SO4−2	−0.0365	Freyer and Voigt (2004)
Cl− K+ Mg+2	−0.022 −14.27	Bischofite/Carnallite/Sylvite, Linke and Seidell (1958)
Cl− K+ Na+	−0.0015 0 0 1.8e−5	Halite/Sylvite solubilities, Linke and Seidell (1958)
Cl− K+ SO4−2	−1e−3	Arcanite/Sylvite solubilities, Linke and Seidell (1958)
Cl− Mg+2 Na+	−0.012 −9.51	Bischofite/Halite/MgSO4·nH2O, Linke and Seidell (1958), Pabalan and Pitzer (1987)
Cl− Mg+2 SO4−2	−0.008 32.63	Bischofite/MgSO4·nH2O, Linke and Seidell (1958)
Cl− Na+ SO4−2	0	Halite/Mirabilite/Thenardite solubilities, Linke and Seidell (1958)
Cl− HCO3− Na+	0 0 0 2.19e−4	Ellis (1963), Wolf et al. (1989)
−THETA		
Ba+2 Na+	0.07	Blount (1977), Templeton (1960)
Ca+2 K+	−5.35e−3 0 0 3.08e−4	Freyer and Voigt (2004)
Ca+2 Na+	9.22e−2 0 0 −4.29e−4 1.21e−6	Block and Waters (1968), Blount and Dickson (1969), Freyer and Voigt (2004)
Cl− SO4−2	0.03	Block and Waters (1968), Blount and Dickson (1969), Freyer and Voigt (2004)

Table 1 (*continued*)

Pitzer term, solute species	A0 .. A5	References
−LAMDA		
H4SiO4 SO4−2	−0.085 0 0.28 −8.25e−4	Marshall and Warakomski (1980), Chen and Marshall (1982)
H4SiO4 Na+	0.0566 75.3 0.115	Marshall and Warakomski (1980), Chen and Marshall (1982)
H4SiO4 Mg+2	0.238 −1788 −9.023 0.0103	Marshall and Warakomski (1980), Chen and Marshall (1982)
Ca+2 H4SiO4	0.238	Marshall and Warakomski (1980)
H4SiO4 K+	2.98e−2	Marshall and Warakomski (1980)
H4SiO4 Li+	0.143	Marshall and Warakomski (1980)
−ZETA		
Cl− H4SiO4 K+	−0.0153	Marshall and Warakomski (1980)
Cl− H4SiO4 Li+	−0.0196	Marshall and Warakomski (1980)
H4SiO4 K+ NO3−	−0.0153	Marshall and Warakomski (1980)
H4SiO4 Li+ NO3−	−8e−3	Marshall and Warakomski (1980)

5. Activity and fugacity coefficients

5.1. Gases

The activity of a gas is its pressure divided by the standard pressure and multiplied with the fugacity coefficient. For example for CO_2:

$$[P_{CO_2}] = \frac{P_{CO_2}}{1\ \text{atm}}\varphi_{CO_2}, \tag{10}$$

where the square brackets indicate activity (–) and φ is the fugacity coefficient (–). The fugacity coefficient can be obtained by comparing the ideal gas law with an equation of state for the gas (Redlich and Kwong, 1949). General equations of state use the acentric factor (Soave, 1972; Peng and Robinson, 1976) in addition to Van der Waals' a and b factors:

$$P = \frac{RT}{V_m - b} - \frac{a\alpha}{V_m^2 + 2bV_m - b^2}, \tag{11}$$

where V_m is the molar volume (cm^3/mol), b is the minimal molar volume (cm^3/mol), a is the Van der Waals' attraction (atm cm^3/mol) and α is the acentric factor (–). a and b can be calculated from the critical temperature and pressure of the gas (Peng and Robinson, 1976). From Eq. (11), the fugacity coefficient is:

$$\ln(\varphi) = \left(\frac{PV_m}{RT} - 1\right) - \ln\left(\frac{P(V_m - b)}{RT}\right) + \frac{a\alpha}{2.828bRT} \times \ln\left(\frac{V_m + 2.414b}{V_m - 0.414b}\right). \tag{12}$$

For CO_2, the fugacity coefficient calculated with Eq. (12) and Peng–Robinson parameters agrees excellently with Duan et al.'s (2006) model at low temperatures and pressures (Appelo et al., 2014). Also for higher temperatures and pressures, the model data from Angus et al. (1976) and Peng and Robinson (1976) agree very well, as shown in Fig. 4.

With the activity (or fugacity) of the gas known from the equation of state, the solubility can be calculated with Henry's law. For CO_2:

$$m_{CO_2} = \frac{[P_{CO_2}]}{\gamma_{CO_2}} K_H \exp\left(\frac{-V_{m\ CO_2,aq}(P-1)}{RT}\right), \tag{13}$$

where K_H is Henry's constant (mol/kgw), corrected for temperature by a polynomial. As shown in the appendix, the interaction parameters among CO_2 and the major ions given by Harvie et al. (1984) for 25 °C can be applied as such for temperatures up to 300 °C in NaCl solutions (data from Drummond, 1981; Rumpf et al., 1994), 140 °C in Na_2SO_4 solutions (data from Rumpf and Maurer, 1993), and 120 °C in $CaCl_2$ solutions (data from Springer et al., 2012). Springer et al. (2012) modeled the same data, and also with temperature-invariant interaction parameters of CO_2 and cations in solution. Thus, the temperature dependence used by He and Morse (1993), Duan and Sun (2003), Duan and Li (2008), is not really necessary, but compensates the formulas that these authors use for calculating the fugacity coefficient and/or the aqueous molar volume of CO_2.

5.2. Aqueous solution

The activity of a solute species is its (analyzed) total molality minus complexes, divided by 1 mol/kgw, multiplied with the activity coefficient. For example for Ca^{2+}:

$$\left[Ca^{2+}\right] = \frac{\gamma_{Ca^{2+}} m_{Ca^{2+}}}{m^0} = \frac{\gamma_{Ca^{2+}}(m_{Ca,total} - m_{Ca-complexes})}{m^0} \tag{14}$$

where γ is the activity coefficient (–) and m^0 is the standard state (1 mol/kgw). In dilute solutions, the activity coefficient decreases with ionic strength according to the Debye-Hückel equation:

$$\ln\gamma_i = -A_\gamma z_i^2 \left(\frac{I^{0.5}}{1 + \mathring{a}B_\gamma I^{0.5}}\right) \tag{15}$$

where z is the charge number, $\mathring{a}$ is the ion-size parameter (Å), and A_γ and B_γ are the Debye-Hückel parameters given by:

$$B_\gamma = \frac{F}{10^{10}}\sqrt{\frac{2\rho}{\varepsilon_0\varepsilon_r RT}} \quad \text{and} \quad A_\gamma = \frac{F^3}{8\pi N_A}\sqrt{\frac{2\rho}{(\varepsilon_0\varepsilon_r RT)^3}} \tag{16}$$

where F is the Faraday constant (96,485 C/mol), ρ is the density of water (kg/m^3), ε_0 is the permittivity of vacuum (8.854e-12 C^2/N/m^2), ε_r is the relative permittivity of water (78.5 at 25 °C). The units of A_γ and B_γ are Å^{-1} (mol/kg)$^{-0.5}$ and (mol/kg)$^{-0.5}$, respectively. The Debye-Hückel equation is for long-range, electrostatic interactions in a medium with continuum properties. Short range interactions are introduced by adding a bI term to Eq. (15) and the association of ions in solute complexes.

In Pitzer models, the Debye-Hückel term is:

$$\ln\gamma_i = -\frac{A_\gamma z_i^2}{3}\left(\frac{I^{0.5}}{1 + bI^{0.5}} + \frac{2}{b}\ln\left(1 + bI^{0.5}\right)\right) \tag{17}$$

where b is selected to be 1.2 (mol/kg)$^{-0.5}$. The short-range interactions are accounted for by adding various terms to Eq. (17) and possibly, complexes (Pitzer, 1986; Harvie et al., 1984).

Pitzer (1986) states that Eq. (17), with b = 1.2, is valid for the full range of applicability of this type of equation, independent of T, P or solute type. Equations (15) and (17) give the same results indeed, at 25 °C and 1–1000 atm, with $\mathring{a}$ = 2 Å. However, Eq. (17) lacks the Debye-Hückel B_γ parameter, which depends on the dielectric constant of water, and changes a little, but significantly, with temperature and pressure. Furthermore, $\mathring{a}$ is higher than 2 Å

Table 2
Minerals used for obtaining Pitzer interaction coefficients, and the polynomial terms for calculating their solubility as a function of temperature, log K = A0 + A1 × T + A2/T + A3 × log T + A4/T^2 + A5 × T^2.

Mineral	A0 ... A5	References
Anhydrite CaSO4 = Ca+2 + SO4−2	5.009 −2.21e−2 −796.4	Block and Waters (1968), Blount and Dickson (1969), Freyer and Voigt (2004)
Arcanite K2SO4 = SO4−2 + 2K+	674.142 0.30423 −18,037 −280.236 0 −1.44055e−4*	Linke and Seidell (1958)
Barite BaSO4 = Ba+2 + SO4−2	−282.43 −8.972e−2 5822 113.08	Blount (1977), Templeton (1960)
Bischofite MgCl2:6H2O = Mg+2 + 2Cl− + 6H2O	7.526 −1.114e−2 115.7	Linke and Seidell (1958)
Carnallite KMgCl3:6H2O = K+ + Mg++ + 3Cl− + 6H2O	24.06 −3.11e−2 −3.09e3	Linke and Seidell (1958)
Epsomite MgSO4:7H2O = Mg+2 + SO4−2 + 7H2O	4.479 −6.99e−3 −1.265e3	Linke and Seidell (1958)
Glauberite Na2Ca(SO4)2 = Ca+2 + 2Na+ + 2SO4−2	218.142 0 −9285 −77.735	Block and Waters (1968), Freyer and Voigt (2004)
Goergeyite K2Ca5(SO4)6H2O = 2K+ + 5Ca+2 + 6SO4−2 + H2O	1056.787 0 −52,300 −368.06	Freyer and Voigt (2004)
Gypsum CaSO4:2H2O = Ca+2 + SO4−2 + 2H2O	82.381 0 −3804.5 −29.9952	Block and Waters (1968), Blount and Dickson (1969), Freyer and Voigt (2004)
Halite NaCl = Cl− + Na+	159.605 8.4294e−2 −3975.6 −66.857 0 −4.9364e−5	Pabalan and Pitzer (1987), Clarke and Glew (1985)
Hexahydrite MgSO4:6H2O = Mg+2 + SO4−2 + 6H2O	−0.733 −2.80e−3 −8.57e−3	Linke and Seidell (1958)
Kalicinite KHCO3 = K+ + H+ + CO3−2	−9.94	Harvie et al. (1984)
Kieserite MgSO4:H2O = Mg+2 + SO4−2 + H2O	47.24 −0.12077 −5.356e3 0 0 7.272e−5	Linke and Seidell (1958)
MgCl2_2H2O MgCl2:2H2O = Mg+2 + 2Cl− + 2H2O	−10.273 0 7.403e3	Linke and Seidell (1958)
MgCl2_4H2O MgCl2:4H2O = Mg+2 + 2Cl− + 4H2O	12.98 −2.013e−2	Linke and Seidell (1958)
Mirabilite Na2SO4:10H2O = SO4−2 + 2Na+ + 10H2O	−301.9326 −0.16232 0 141.078	Linke and Seidell (1958)
SiO2(a) SiO2 + 2 H2O = H4SiO4	20.42 3.107e−3 −1492 −7.68	Chen and Marshall (1982)
Sylvite KCl = K+ + Cl−	−50.571 9.8815e−2 1.3135e4 0 −1.3754e6 −7.393e−5	Linke and Seidell (1958)
Syngenite K2Ca(SO4)2:H2O = 2K+ + Ca+2 + 2SO4−2 + H2O	log_k −6.43; −delta_h −32.65**	Freyer and Voigt (2004)
Thenardite Na2SO4 = 2 Na+ + SO4−2	57.185 8.6024e−2 0 −30.8341 0 −7.6905e−5	Pabalan and Pitzer (1987)

* The Linke and Seidell data for arcanite may give subsaturation in other experiments, SI = −0.06.
** The Van't Hoff equation is used for syngenite.

for most ions. The result is, that γ's increase relatively more with pressure in Pitzer models than with the Debye-Hückel equation. This is illustrated in Fig. 5A for 6 M NaCl at 25 and 200 °C. The relative increase of the Pitzer's gammas counteracts the increase of solubility with pressure and gives too small solubilities, as shown for halite in Fig. 5B. It is possible to introduce the Debye-Hückel formula in the Pitzer calculation, but then the whole database must be re-optimized. More ad-hoc, the effect can be balanced by changing b for monovalent species to:

$$b = 1.2 - (7e-5 + 1.93e-9 \times (T-250)^2) \times P \quad (18)$$

and for divalent species to:

$$b = 1.2 - (9.65e-10 \times (T-263)^{2.773}) \times P^{0.623}, \quad (19)$$

with $b > 1$. The equations were obtained by optimizing solubilities of halite and sulfates.

6. Extending the Pitzer database to higher temperatures

Following the leads of Harvie and Weare (1980), Weare (1987), Pabalan and Pitzer (1987), the pitzer.dat database was extended to higher temperatures using (1) osmotic coefficients from vapor pressure measurements and (2) solubilities of various salts. In the latter case, the numbers were obtained stepwise, starting with (2a) interaction coefficients and the temperature-dependent polynomial for the solubility from binary solutions, and then, (2b) finding other interaction coefficients from the solubility in multicomponent solutions.

All the Pitzer interaction coefficients were refitted on the data, since parameters may be inconsistent (for example, the Pitzer variable α_1 used for Na_2SO_4(aq) by Holmes and Mesmer (1986) is different from the usual value of 2), or since parameterizations are invalid outside the range used for fitting the parameters (for example, the $CaSO_4$–Na_2SO_4 model from Greenberg and Møller (1989) deviates at 200 °C as shown by Freyer and Voigt (2004), see Fig. 6 in this paper). The experimental data were digitized from graphs or tables and are part of a set of input files given as electronic appendix. As noted in the 'Principles' and 'Tools' sections, the number of parameters and the number of digits used for the parameters were minimized. Tables 1 and 2 give the resulting set of Pitzer parameters, and the polynomials for the temperature dependence of the solubility of salts, respectively, with references to the data used for fitting.

Briefly, the polynomial terms for Na–K–Mg–Cl–SO_4 collected by Pabalan and Pitzer (1987) were translated into PHREEQC polynomials, except for Na^+–Cl^-, which were refitted on the numbers from Pitzer et al., 1984, Table A1, without the P terms. Also, K^+–SO_4^{-2} and Na^+–SO_4^{-2} were fitted on the osmotic coefficients from

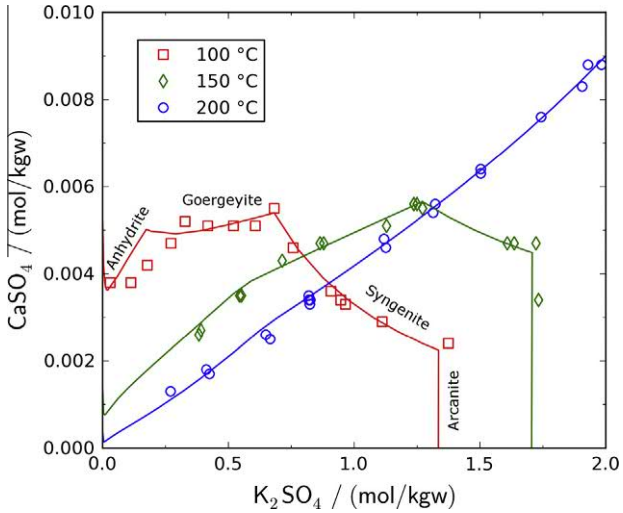

Fig. 7. Solubilities of anhydrite, goergeyite, syngenite and arcanite at 100, 150 and 200 °C. Data points from Freyer and Voigt (2004), with model lines from the Pitzer model.

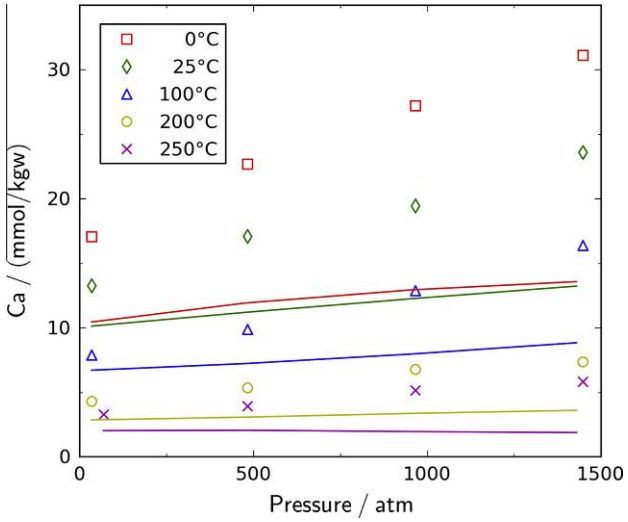

Fig. 8. Solubility of calcite in 4 M NaCl solution at various temperatures as a function of pressure. Data points from Shi et al. (2013).

Holmes and Mesmer (1986) since they used $\alpha_1 = 1.4$, instead of 2, and B1 numbers are much different from the usual numbers in pitzer.dat. Added were the Ca^{+2}–Cl^- coefficients using the data listed by Holmes et al. (1994), and the interaction coefficients of Ca^{+2} with other ions were obtained using solubility data. The interaction coefficients of HCO_3^- with other ions were found using solubility data of calcite, and checked with the figures of Harvie et al. (1984) at 25 °C. Finally, the coefficients for Ba^{+2} and H_4SiO_4 were added, again using solubility data.

As examples, the experimental solubilities of anhydrite, glauberite and thenardite, established by Freyer and Voigt (2004), are shown in Fig. 6 at 100, 150 and 200 °C as functions of the Na_2SO_4 and $CaSO_4$ concentration, together with model lines from the Pitzer model presented in Tables 1 and 2, and from Greenberg and Møller's (1989) model that is correct at 100 °C, but largely underestimates the solubility of anhydrite and glauberite at 200 °C. Freyer and Voigt (2004) also determined solubilities in the K–Ca–SO_4 system at 100, 150 and 200 °C, and also these can be modeled well with the Pitzer model presented here, as shown in Fig. 7. Solubility plots for more sulfates, chlorides, carbonates and amorphous silica are shown in the appendix, as listed in Table 3.

7. Remaining pitfalls and missing data

Although it has been shown that many data can be modeled well with the modified Pitzer database, it is also fair to mention that some experiments cannot. Shi et al. (2013) measured the calcite solubility in 0.1 M and 4 M NaCl and 1 bar CO_2 pressure at temperatures from 0 to 250 °C and 1 to 1450 atm pressure, as shown in Fig. 8. The model lines diverge considerably from the

Table 3
List of figures with mineral solubilities as a function of *T*, *P* and solution composition given in the Appendix (Supporting Information file). Input files for calculating the plots with PHREEQC and the adapted Pitzer model can be downloaded from www.hydrochemistry.eu. The data are from measurements and compilations by: Angus et al. (1976), Block and Waters (1968), Blount and Dickson (1969, 1973), Blount (1977), Chen and Marshall (1982), Clarke and Glew (1985), Drummond (1981), Ellis (1959, 1963), Freyer and Voigt (2004), King et al. (1992), Linke and Seidell (1958), Malinin and Kanukov (1971), Marshall and Slusher (1966), Marshall and Warakomski (1980), Miller (1952), Pabalan and Pitzer (1987), Plummer and Busenberg (1982), Rumpf and Maurer (1993), Rumpf et al. (1994), Shi et al. (2013), Springer et al. (2012), Takenouchi and Kennedy (1964), Templeton (1960), Uchameyshvili et al. (1966), Wiebe and Gaddy (1939, 1940), Wolf et al. (1989).

Mineral solubility in water or aqueous solution	Temp °C	Pressure/atm	Figures
Halite (NaCl)	0–300	1–P_{sat}	A1
Sylvite (KCl)	10–300	1–P_{sat}	A2
Bischofite ($MgCl_2$:$6H_2O$), $MgCl_2$:$2H_2O$, $MgCl_2$:$4H_2O$	0–200	1–P_{sat}	A3
Mirabilite (Na_2SO_4:$10H_2O$), thenardite (Na_2SO_4)	0–220	1–P_{sat}	A4
Arcanite (K_2SO_4)	0–210	1–P_{sat}	A5
Epsomite ($MgSO_4$:$7H_2O$), hexahydrite ($MgSO_4$:$6H_2O$), kieserite ($MgSO_4$:H_2O)	0–200	1–P_{sat}	A6
Halite (NaCl), sylvite (KCl) in Na/K–Cl solutions	0–200	1–P_{sat}	A7
Carnallite ($KMgCl_3$:H_2O) in K/Mg–Cl solutions	0–75	1	A8
Gypsum ($CaSO_4$:$2H_2O$)	0–95	1	A9
Gypsum ($CaSO_4$:$2H_2O$) in NaCl solutions	0.5–95	1	A10
Gypsum ($CaSO_4$:$2H_2O$), mirabilite (Na_2SO_4:$10H_2O$), glauberite ($Na_2Ca(SO_4)_2$) and thenardite (Na_2SO_4) in Na_2SO_4 solutions	25–100	1	A11
Gypsum ($CaSO_4$:$2H_2O$) and anhydrite ($CaSO_4$)	30–160	1–1000	A12
Anhydrite ($CaSO_4$) in NaCl solutions	100–200	1–P_{sat}	A13
Anhydrite ($CaSO_4$) in NaCl solutions	100–200	1–987	A14
Anhydrite ($CaSO_4$) and glauberite ($Na_2Ca(SO_4)_2$) in Na_2SO_4 solutions	100–200	1–P_{sat}	A15
Anhydrite ($CaSO_4$), Goergeyite ($K_2Ca_5(SO_4)_6H_2O$) and syngenite ($K_2Ca(SO4)_2$:H_2O) in K_2SO_4 solutions	100–200	1–P_{sat}	A16
Amorphous silica (SiO_2(a)) in NaCl solutions	25–300	1–P_{sat}	A17
Amorphous silica (SiO_2(a)) in Na_2SO_4 solutions	25–300	1–P_{sat}	A18
Amorphous silica (SiO_2(a)) in $MgCl_2$ solutions	25–300	1–P_{sat}	A19
Amorphous silica (SiO_2(a)) in $MgSO_4$ solutions	25–250	1–P_{sat}	A20
Amorphous silica (SiO_2(a)) in Li–Cl/NO_3 solutions	25	1	A21
Amorphous silica (SiO_2(a)) in K–Cl/NO_3 solutions	25	1	A22
Amorphous silica (SiO_2(a)) in $CaCl_2$ solutions	25	1	A23
Barite ($BaSO_4$) in NaCl solutions	1–250	1–P_{sat}	A24
Barite ($BaSO_4$) in NaCl solutions	150–250	493	A25
Calcite ($CaCO_3$) in NaCl solutions	10–60	1	A26
Calcite ($CaCO_3$) in 3 M NaCl, variable CO_2	200	580	A27
Calcite ($CaCO_3$) in NaCl solutions	120–260	12	A28
Calcite ($CaCO_3$) at 1 bar CO_2 pressure	0–300	1–(P_{sat} + 1)	A29
Calcite ($CaCO_3$) in NaCl solutions at 1 bar CO_2 pressure	0–250	1–1450	A30
CO_2 gas	25–100	1–710	A31
CO_2 gas in 1 and 6 M NaCl solution	25–300	35–200	A32
CO_2 gas in 4 M NaCl solution	80–180	9–95	A33
CO_2 gas in Na_2SO_4 solutions	140	12–96	A34
CO_2 gas in 2.3 M $CaCl_2$ solution	75–120	22–655	A35
CO_2 fugacity coefficients	0–300	99–987	A36

measured solubilities for unknown reasons. The calcite solubility in 0.1 M NaCl solution at the same T and P's can be modeled reasonably well, which makes it difficult to attribute the discrepancy to the experiment.

Furthermore, the calculation of the solubility of aluminosilicates requires the inclusion of Al in the database.

8. Conclusions

For ionic strengths higher than 1, the Pitzer interaction model provides an excellent match of measured activity coefficients in aqueous solution. Other databases distributed with PHREEQC do not calculate the mean activity coefficients correctly at high ionic strengths, although they may give correct solubilities in some cases. The model was extended to the 0–200 °C temperature range using mineral solubilities in the Na–K–Mg–Ca–Ba–Cl–CO_2–HCO_3–SO_4–H_4SiO_4 system. The effect of pressure is calculated from the reaction volumes, which, for solutes, are a function of T, P and ionic strength. It was shown that the calculation of the apparent molar volumes of solutes is more efficient than of the partial molar volumes.

Generally, solubilities increase with pressure because the molar volume in solution is smaller than in the minerals. The difference is small for NaCl and consequently, the solubility increase with pressure of halite is small. The small solubility increase could not be captured well with the Pitzer model, because the activity coefficients in solution increase with pressure by the form of the Debye-Hückel equation used by Pitzer, which neglects B_γ. The effect has been countered with a T, P dependent correction, but this solution is rather ad-hoc, and can be improved when data are available. On the other hand, the dielectric properties which determine the change of A_γ and B_γ with pressure are taken from pure water, and their applicability in concentrated solutions is questionable.

The parameters in the model were optimized, redundant parameters were removed, and only significant digits are given in the database. However, the parameters are still highly correlated and usually have mutually compensating effects. For example, it was found that the solubility of CO_2 in saline solutions, at the full pressure and temperature range, could be calculated with the interaction parameters given by Harvie et al. (1984) for 25 °C, whereas other models incorporate temperature- and sometimes pressure-dependent terms. The parameters depend, anyhow, strongly on experimental data, which almost exclusively are obtained in simple salt solutions. Thus, the aim of developing a database for calculating the precipitation of scaling minerals in wells at depths exceeding 4000 m has been given an impetus that will benefit further from practical applications and more experimental results.

Acknowledgements

David Parkhurst has given long-standing support for doing the PHREEQC calculations. Two reviewers are thanked for their notes that were helpful to make the text clear.

Appendix A. Supplementary material

Supplementary data associated with this article can be found, in the online version, at http://dx.doi.org/10.1016/j.apgeochem.2014.11.007.

References

Angus, S., Armstrong, B., De Reuck, K.M. (Eds.), 1976. Carbon Dioxide. Pergamon Press, p. 385.
Appelo, C.A.J., Parkhurst, D.L., Post, V.E.A., 2014. Equations for calculating hydrogeochemical reactions of minerals and gases such as CO_2 at high pressures and temperatures. Geochim. Cosmochim. Acta 125, 49–67.
Atkins, P.W., de Paula, J., 2002. Atkins' Physical Chemistry, seventh ed. Oxford Univ Press, p. 1149.
Block, J., Waters, O.B., 1968. The $CaSO_4$–Na_2SO_4–NaCl–H_2O system at 25–100 °C. J. Chem. Eng. Data 13, 336–344.
Blount, C.W., 1977. Barite solubilities and thermodynamic quantities up to 300°C and 1400 bars. Am. Mineral. 62, 942–957.
Blount, C.W., Dickson, F.W., 1969. The solubility of anhydrite ($CaSO_4$) in NaCl–H_2O from 100 to 450 °C and 1–1000 bars. Geochim. Cosmochim. Acta 33, 227–245.
Blount, C.W., Dickson, F., 1973. Gypsum–anhydrite equilibria in systems $CaSO_4$–H_2O and $CaSO_4$–NaCl–H_2O. Am. Mineral. 58, 323–331.
Chen, C.T.A., Marshall, W.L., 1982. Amorphous silica solubilities IV. Behavior in pure water and aqueous sodium chloride, sodium sulfate, magnesium chloride, and magnesium sulfate solutions up to 350 C. Geochim. Cosmochim. Acta 46, 279–287.
Clarke, E.C.W., Glew, D.N., 1985. Evaluation of the thermodynamic functions for aqueous sodium chloride from equilibrium and calorimetric measurements below 154 C. J. Phys. Chem. Ref. Data 14, 489–610.
Doherty, J., 2003. Groundwater model calibration using pilot points and regularisation. Ground Water 41, 170–177.
Drummond, S.E., 1981. Boiling and mixing of hydrothermal fluids: chemical effects on mineral precipitation. PhD thesis, Penn. State Univ.
Duan, Z., Li, D., 2008. Coupled phase and aqueous species equilibrium of the H_2O–CO_2–NaCl–$CaCO_3$ system from 0 to 250 °C, 1–1000 bar with NaCl concentrations up to saturation of halite. Geochim. Cosmochim. Acta 72, 5128–5145.
Duan, Z., Sun, R., 2003. An improved model calculating CO_2 solubility in pure water and aqueous NaCl solutions from 273 to 533 K and from 0 to 2000 bar. Chem. Geol. 193, 257–271.
Duan, Z., Sun, R., Zhu, C., Chou, I.-M., 2006. An improved model for the calculation of CO_2 solubility in aqueous solutions containing Na^+, K^+, Ca^{2+}, Mg^{2+}, Cl^-, and SO_4^{2-}. Mar. Chem. 98, 131–139.
Ellis, A.J., 1959. The solubility of calcite in carbon dioxide solutions. Am. J. Sci. 257, 354–365.
Ellis, A.J., 1963. Solubility of calcite in sodium chloride solutions at high temperatures. Am. J. Sci. 261, 259–267.
Freyer, D., Voigt, W., 2004. The measurement of sulfate mineral solubilities in the Na–K–Ca–Cl–SO_4–H_2O system at temperatures of 100, 150 and 200 °C. Geochim. Cosmochim. Acta 68, 307–318.
Greenberg, J.P., Møller, N., 1989. The prediction of mineral solubilities in natural waters: a chemical equilibrium model for the Na–K–Ca–Cl–SO_4–H_2O system to high concentration from 0 to 250 °C. Geochim. Cosmochim. Acta 53, 2503–2518.
Harvie, C.E., Weare, J.H., 1980. The prediction of mineral solubilities in natural waters: the Na–K–Mg–Ca–Cl–SO_4–H_2O system from zero to high concentration at 25 °C. Geochim. Cosmochim. Acta 44, 981–997.
Harvie, E.H., Møller, N., Weare, J.H., 1984. The prediction of mineral solubilities in natural waters: the Na–K–Mg–Ca–H–Cl–SO_4–OH–HCO_3–CO_3–CO_2–H_2O system to high ionic strengths at 25 °C. Geochim. Cosmochim. Acta 48, 723–751.
He, S., Morse, J.W., 1993. The carbonic acid system and calcite solubility in aqueous Na–K–Ca–Mg–Cl–SO_4 solutions from 0 to 90 °C. Geochim. Cosmochim. Acta 57, 3533–3554.
Helgeson, H.C., Kirkham, D.H., Flowers, G.C., 1981. Theoretical prediction of the thermodynamic behavior of aqueous electrolytes by high pressures and temperatures: IV. Calculation of activity coefficients, osmotic coefficients, and apparent molal and standard and relative partial molal properties to 600 °C and 5 kb. Am. J. Sci. 281, 1249–1516.
Holmes, H.F., Mesmer, R.E., 1986. Thermodynamics of aqueous solutions of the alkali metal sulfates. J. Sol. Chem. 15, 495–517.
Holmes, H.F., Busey, R.H., Simonson, J.M., Mesmer, R.E., 1994. $CaCl_2$(aq) at elevated temperatures. Enthalpies of dilution, isopiestic molalities, and thermodynamic properties. J. Chem. Thermodynam. 26, 271–298.
Johnson, J.W., Oelkers, E.H., Helgeson, H.C., 1992. SUPCRT92, a software package for calculating the standard molal thermodynamic properties of minerals, gases, aqueous species, and reactions from 1 to 5000 bar and 0 to 1000 °C. Comput. Geosci. 18, 899–947.
Kharaka, Y.K., Gunter, W.D., Aggarwal, P.K., Perkins, E.H., DeBraal, J.D., 1988. SOLMINEQ 88: a computer program for geochemical modelling of water–rock interaction: US. Geol. Surv. Water Resour. Report 88 (4227), 1–420.
King, M.B., Mubarak, A., Kim, J.D., Bott, T.R., 1992. The mutual solubilities of water with supercritical and liquid carbon dioxide. J. Supercrit. Fluids 5, 296–302.
Kulik, D.A., Wagner, T., Dmytrieva, S.V., Kosakowski, G., Chudnenko, K.V., Berner, U., 2012. GEM-Selektor geochemical modeling package: revised algorithm and GEMS3K numerical kernel for coupled simulation codes. Comput. Geosci. 17, 1–24.
Laliberté, M., 2009. A model for calculating the heat capacity of aqueous solutions, with updated density and viscosity data. J. Chem. Eng. Data 54, 1725–1760.
Linke, W.F., Seidell, A., 1958. Solubilities, inorganic and metal–organic compounds. Am. Chem. Soc, 1491.
Malinin, S.D., Kanukov, A.B., 1971. Solubility of calcite in homogeneous H_2O–NaCl–CO_2 systems in 200–600 °C temperature interval. Geochem. Int. 8, 668–679.
Marcus, Y., 2011. Electrostriction in electrolyte solutions. Chem. Rev. 111, 2761–2783.
Marion, G.M., Farren, R.E., 1999. Mineral solubilities in the Na–K–Mg–Ca–Cl–SO_4–H_2O system: a re-evaluation of the sulfate chemistry in the Spencer–Møller–Weare model. Geochim. Cosmochim. Acta 63, 1305–1318.

Marshall, W.L., Slusher, R., 1966. Thermodynamics of calcium sulfate dihydrate in aqueous sodium chloride solutions, 0–110. J. Phys. Chem. 70, 4015–4027.
Marshall, W.L., Warakomski, J.M., 1980. Amorphous silica solubilities—II. Effect of aqueous salt solutions at 25 C. Geochim. Cosmochim. Acta 44, 915–924.
Miller, J.P., 1952. A portion of the system calcium carbonate–carbon dioxide–water, with geological implications. Am. J. Sci. 250, 161–208.
Millero, F.J., 1970. The apparent and partial molal volume of aqueous sodium chloride solutions at various temperatures. J. Phys. Chem. 74, 356–362.
Millero, F.J., 1971. Molal volumes of electrolytes. Chem. Rev. 71, 147–176.
Monnin, C., 1999. A thermodynamic model for the solubility of barite and celestite in electrolyte solutions and seawater to 200 °C and to 1 kbar. Chem. Geol. 153, 187–209.
Pabalan, R.T., Pitzer, K.S., 1987. Thermodynamics of concentrated electrolyte mixtures and the prediction of mineral solubilities to high temperatures for mixtures in the system Na–K–Mg–Cl–SO_4–OH–H_2O. Geochim. Cosmochim. Acta 51, 2429–2443.
Parkhurst, D.L., Appelo, C.A.J., 2013. Description of input and examples for PHREEQC Version 3—a computer program for speciation, batch-reaction, one-dimensional transport, and inverse geochemical calculations. U.S. Geol. Surv. Techn. Methods Report, book 6, chapter A43, p. 497.
Peng, D.-Y., Robinson, D.B., 1976. A new two-constant equation of state. Ind. Eng. Chem. Fund. 15, 59–64.
Pitzer, K.S., 1986. Theoretical considerations of solubility with emphasis on mixed aqueous electrolytes. Pure Appl. Chem. 58, 1599–1610.
Pitzer, K.S., Peiper, J.C., Busey, R.H., 1984. Thermodynamic properties of aqueous sodium chloride solutions. J. Phys. Chem. Ref. Data 13, 1–102.
Plummer, L.N., Busenberg, E., 1982. The solubilities of calcite, aragonite and vaterite in CO_2–H_2O solutions between 0 °C and 90 °C, and an evaluation of the aqueous model for the system $CaCO_3$–CO_2–H_2O. Geochim. Cosmochim. Acta 46, 1011–1040.
Plummer, L.N., Parkhurst, D.L., Fleming, G.W., Dunkle, S.A., 1988. A computer program incorporating Pitzer's equations for calculation of geochemical reactions in brines. U.S. Geological Survey Water-Resources Investigations Report 88–4153, p. 310.
Redlich, O., Kwong, J., 1949. On the thermodynamics of solutions. V. An equation of state. Fugacities of gaseous solutions. Chem. Rev. 44, 233–244.
Redlich, O., Rosenfeld, P., 1931. The theory of the molal volume of a dissolved electrolyte. II. Z. Elektrochem. Angew. P. 37, 705.
Robinson, R.A., Stokes, R.H., 1959. Electrolyte solutions, second ed. Butterworths, London, p. 559.
Rumpf, B., Maurer, G., 1993. An experimental and theoretical investigations on the solubility of carbon dioxide in aqueous solutions of strong electrolytes. Ber. Bunsenges. Phys. Chem. 97, 85–97.
Rumpf, B., Nicolaisen, H., Öcal, C., Maurer, G., 1994. Solubility of carbon dioxide in aqueous solutions of sodium chloride: experimental results and correlation. J. Solution Chem. 23, 431–448.
Shi, W., Kan, A.T., Zhang, N., Tomson, M., 2013. Dissolution of calcite at up to 250 °C and 1450 bar and the presence of mixed salts. Ind. Eng. Chem. Res. 52, 2439–2448.
Soave, G., 1972. Equilibrium constants from a modified Redlich-Kwong equation of state. Chem. Eng. Sci. 27, 1197–1203.
Springer, R.D., Wang, Z., Anderko, A., Wang, P., Felmy, A.R., 2012. A thermodynamic model for predicting mineral reactivity in supercritical carbon dioxide: I. Phase behavior of carbon dioxide–water–chloride salt systems across the H_2O-rich to the CO_2-rich regions. Chem. Geol. 322–323, 151–171.
Takenouchi, S., Kennedy, G.C., 1964. The binary system H_2O–CO_2 at high temperatures and pressures. Am. J. Sci. 262, 1055–1074.
Templeton, C.C., 1960. Solubility of barium sulfate in sodium chloride solutions from 25° to 95 °C. J. Chem. Eng. Data 5, 514–516.
Uchameyshvili, N.Y., Malinin, S.D., Khitarov, N.I., 1966. Solubility of barite in concentrated chloride solutions of some metals at elevated temperatures in relation to problems of the genesis of barite deposits. Geochem. Int. 10, 951–963.
Villafáfila García, A., 2005. Measurement and modeling of scaling minerals. PhD thesis, Technical University of Denmark, p. 230.
Weare, J.H., 1987. Models of mineral solubility in concentrated brines with application to field observations. Rev. Mineral. Geochem. 17, 143–176.
Wiebe, R., Gaddy, V.L., 1939. The solubility in water of carbon dioxide at 50°, 75° and 100 °C at pressures to 700 atm. J. Am. Chem. Soc. 61, 315–318.
Wiebe, R., Gaddy, V.L., 1940. The solubility of carbon dioxide in water at various temperatures from 12 to 40° and at pressures to 500 atm. J. Am. Chem. Soc. 62, 815–817.
Wolf, M., Breitkopf, O., Puk, R., 1989. Solubility of calcite in different electrolytes at temperatures between 10 and 60 °C and at CO_2 partial pressures of about 1 kPa. Chem. Geol. 76, 291–301.

Appendix to:
C.A.J. Appelo, Principles, caveats and improvements in databases for calculating hydrogeochemical reactions in saline waters from 0 - 200 ºc and 1 - 1000 atm.

This appendix has figures showing experimental solubilities and PHREEQC calculations, using the Pitzer interaction coefficients given in Table 1, and the temperature dependent log *K*'s in Table 2 of the paper. The PHREEQC input files are in the directory:
c:\phreeqc\high_P_T\appendix_AG15
The main directory contains pitzer.dat and input files that calculate the figures presented by Pabalan and Pitzer, 1987. Input files for other minerals and CO_2 gas are in sub-directories.
It is easiest to run the files with Notepad++ adapted for PHREEQC. Download from:
http://www.hydrochemistry.eu/ph3/phreeqc3.Installer.exe
and install in your computer. In Notepad++, open a file (Ctrl+O), and press Ctrl+F6 to start the PHREEQC calculations.

Table 3. List of figures with mineral solubilities as a function of *T, P* and solution composition.

Mineral solubility in water or aqueous solution	Temp ºC	Pressure / atm	Figure
halite (NaCl)	0 - 300	1 - P_{sat}	A1
sylvite (KCl)	10 - 300	1 - P_{sat}	A2
bischofite ($MgCl_2$:$6H_2O$), $MgCl_2$:$2H_2O$, $MgCl_2$:$4H_2O$	0 - 200	1 - P_{sat}	A3
mirabilite (Na_2SO_4:$10H_2O$), thenardite (Na_2SO_4)	0 - 220	1 - P_{sat}	A4
arcanite (K_2SO_4)	0 - 210	1 - P_{sat}	A5
epsomite ($MgSO_4$:$7H_2O$), hexahydrite ($MgSO_4$:$6H_2O$), kieserite ($MgSO_4$:H_2O)	0 - 200	1 - P_{sat}	A6
halite (NaCl), sylvite (KCl) in Na/K-Cl solutions	0 - 200	1 - P_{sat}	A7
carnallite ($KMgCl_3$:H_2O) in K/Mg-Cl solutions	0 - 75	1	A8
gypsum ($CaSO_4$:$2H_2O$)	0 - 95	1	A9
gypsum ($CaSO_4$:$2H_2O$) in NaCl solutions	0.5 - 95	1	A10
gypsum ($CaSO_4$:$2H_2O$), mirabilite (Na_2SO_4:$10H_2O$), glauberite ($Na_2Ca(SO_4)_2$) and thenardite (Na_2SO_4) in Na_2SO_4 solutions	25 - 100	1	A11
gypsum ($CaSO_4$:$2H_2O$) and anhydrite ($CaSO_4$)	30 - 160	1 - 1000	A12
anhydrite ($CaSO_4$) in NaCl solutions	100 - 200	1 - P_{sat}	A13
anhydrite ($CaSO_4$) in NaCl solutions	100 - 200	1 - 987	A14
anhydrite ($CaSO_4$) and glauberite ($Na_2Ca(SO_4)_2$) in Na_2SO_4 solutions	100 - 200	1 - P_{sat}	A15
anhydrite ($CaSO_4$), Goergeyite ($K_2Ca_5(SO_4)_6H_2O$) and syngenite ($K_2Ca(SO4)_2$:H_2O) in K_2SO_4 solutions	100 - 200	1 - P_{sat}	A16
amorphous silica (SiO_2(a)) in NaCl solutions	25 - 300	1 - P_{sat}	A17
amorphous silica (SiO_2(a)) in Na_2SO_4 solutions	25 - 300	1 - P_{sat}	A18
amorphous silica (SiO_2(a)) in $MgCl_2$ solutions	25 - 300	1 - P_{sat}	A19
amorphous silica (SiO_2(a)) in $MgSO_4$ solutions	25 - 250	1 - P_{sat}	A20
amorphous silica (SiO_2(a)) in Li-Cl/NO_3 solutions	25	1	A21

amorphous silica (SiO_2(a)) in K-Cl/NO_3 solutions	25	1	A22
amorphous silica (SiO_2(a)) in $CaCl_2$ solutions	25	1	A23
barite ($BaSO_4$) in NaCl solutions	1 - 250	1 - P_{sat}	A24
barite ($BaSO_4$) in NaCl solutions	150 - 250	493	A25
calcite ($CaCO_3$) in NaCl solutions	10 - 60	1	A26
calcite ($CaCO_3$) in 3 M NaCl, variable CO_2	200	580	A27
calcite ($CaCO_3$) in NaCl solutions	120 - 260	12	A28
calcite ($CaCO_3$) at 1 bar CO_2 pressure	0 - 300	1 - (P_{sat}+1)	A29
calcite ($CaCO_3$) in NaCl solutions at 1 bar CO_2 pressure	0 - 250	1 - 1450	A30
CO_2 gas	25 - 100	1 - 710	A31
CO_2 gas in 1 and 6 M NaCl solution	25 - 300	35 - 200	A32
CO_2 gas in 4 M NaCl solution	80 - 180	9 - 95	A33
CO_2 gas in Na_2SO_4 solutions	140	12 - 96	A34
CO_2 gas in 2.3 M $CaCl_2$ solution	75 - 120	22 - 655	A35
CO_2 fugacity coefficients	0 - 300	99 - 987	A36

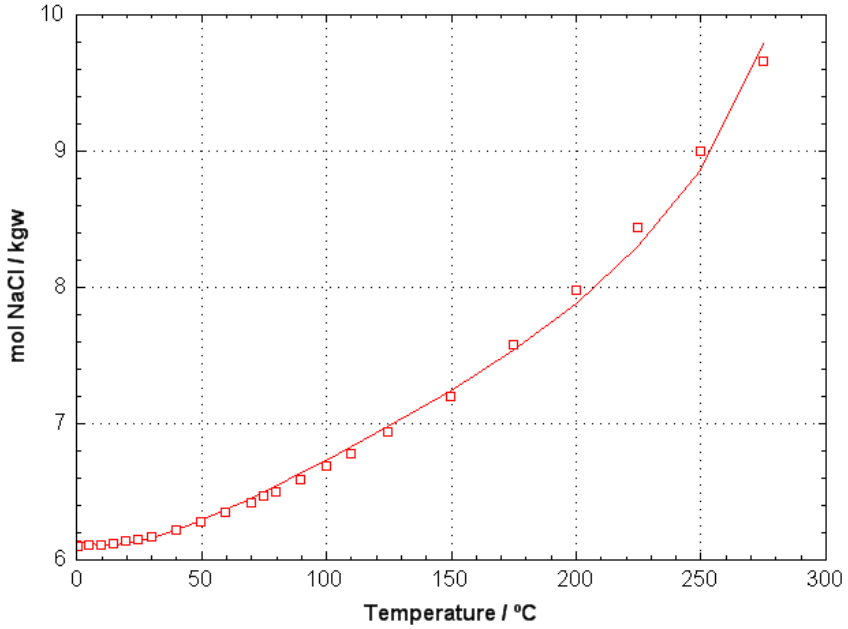

Figure A1. Halite (NaCl) solubility as a function of temperature. Data points from Pabalan and Pitzer, 1987; Clarke and Glew, 1985. File Halite.phr

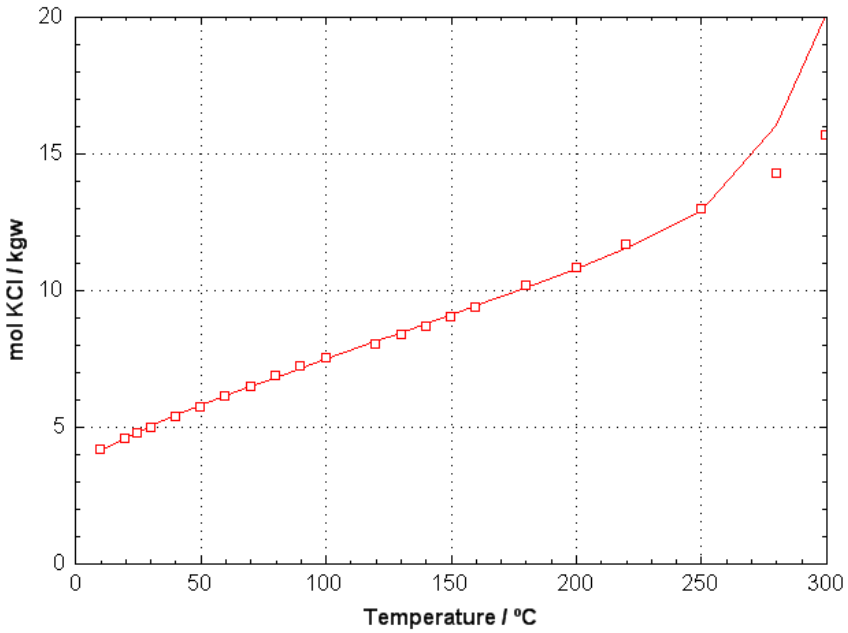

Figure A2. Sylvite (KCl) solubility as a function of temperature. Data points from Pabalan and Pitzer, 1987. File Sylvite.phr

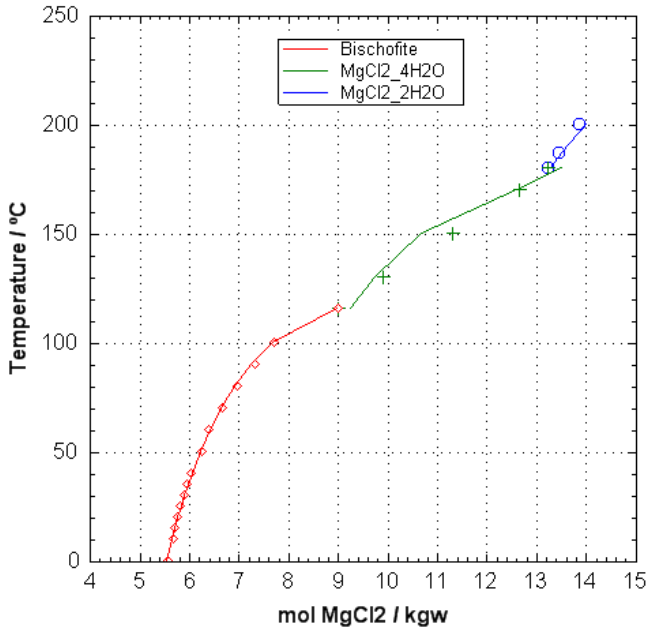

Figure A3. Solubility of $MgCl_2$-hydrates. Data points from Pabalan and Pitzer, 1987. File $MgCl_2$.phr

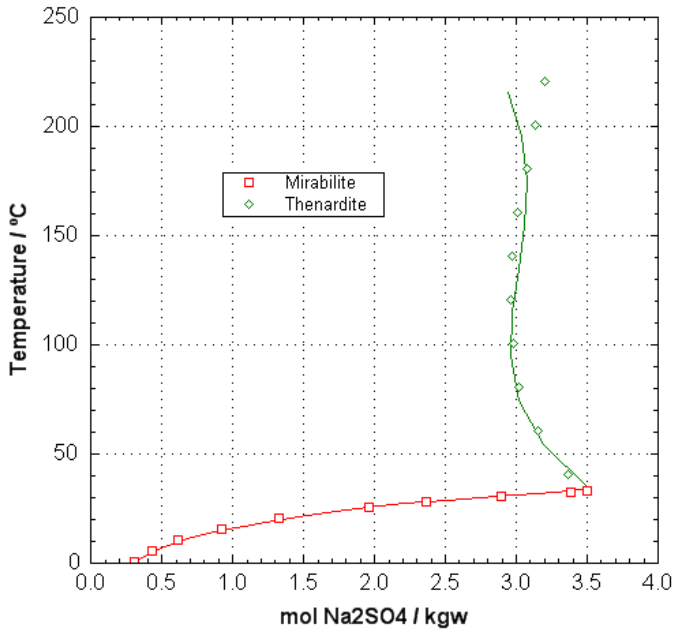

Figure A4. Solubility of Na_2SO_4-(an)hydrate. Data points from Pabalan and Pitzer, 1987. File Na2SO4.phr

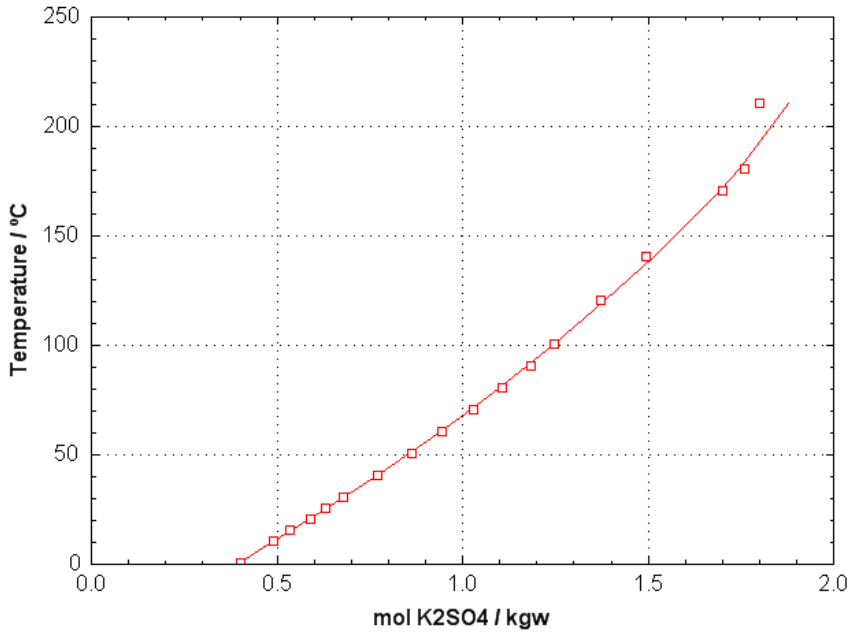

Figure A5. Solubility of arcanite (K_2SO_4). Data points from Pabalan and Pitzer, 1987. File K2SO4.phr

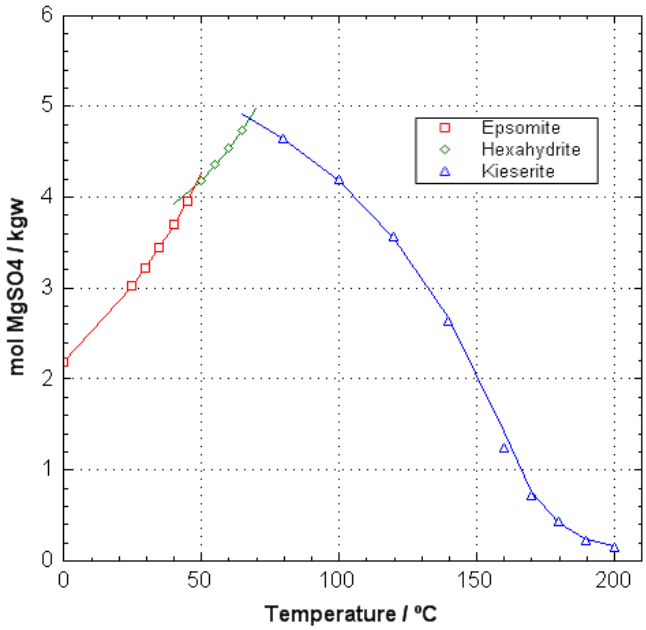

Figure A6. Solubility of $MgSO_4$-hydrates. Data points from Pabalan and Pitzer, 1987. File MgSO4.phr

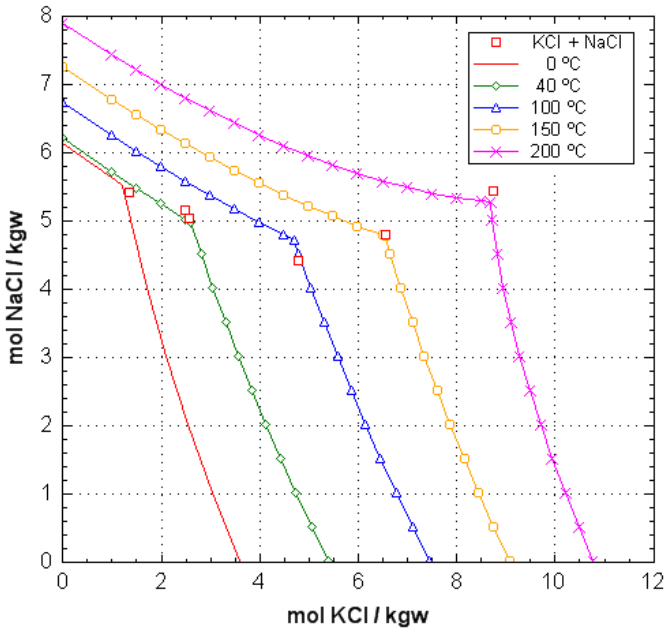

Figure A7. Mutual influence of NaCl and KCl solutions on halite and sylvite solubilities, with triple points KCl + NaCl + H_2O from Pabalan and Pitzer, 1987. File NaKCl.phr

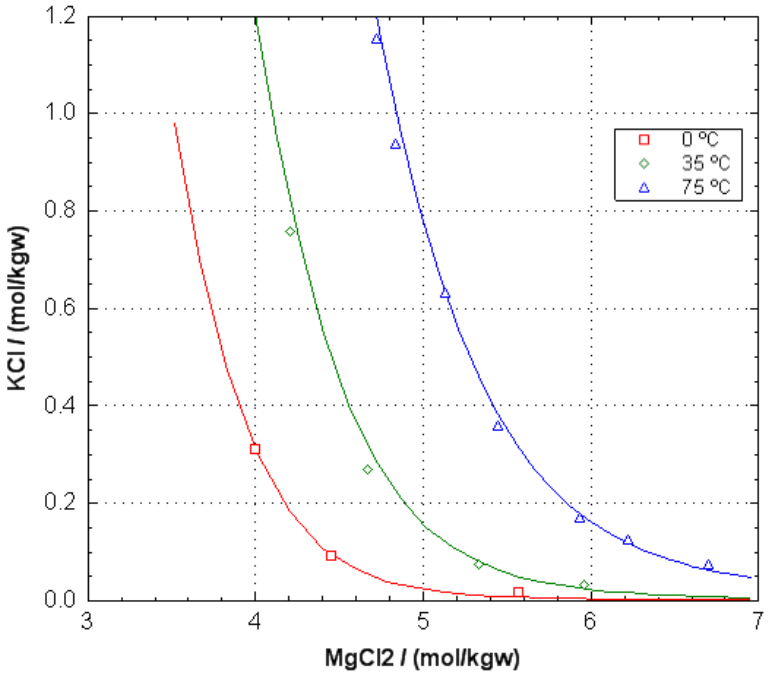

Figure A8. Solubility of carnallite ($KMgCl_3$:H_2O). Data points from Pabalan and Pitzer, 1987. File Carnallite.phr

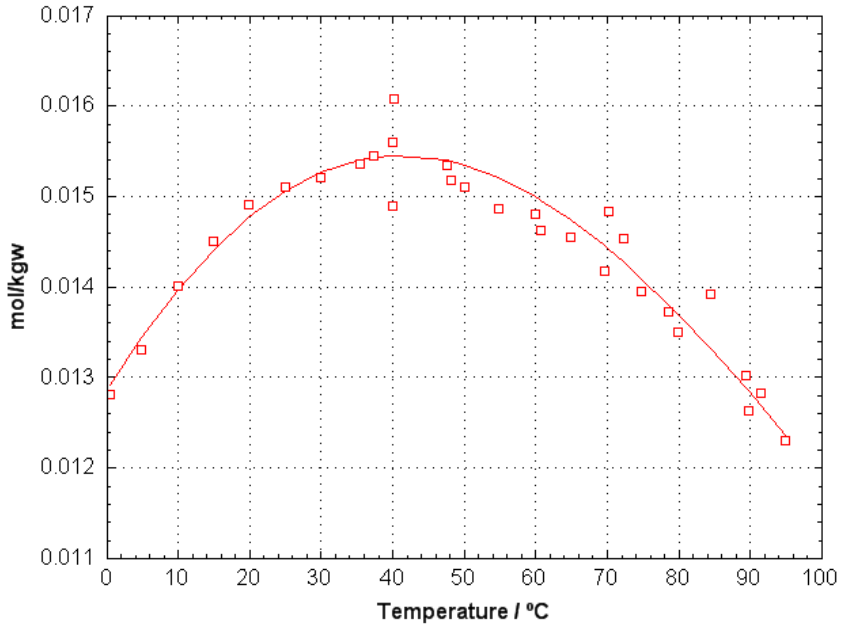

Figure A9. Solubility of gypsum ($CaSO_4:2H_2O$). Data points from Marshall and Slusher, 1966; Blount and Dickson, 1969. File gypsum.phr

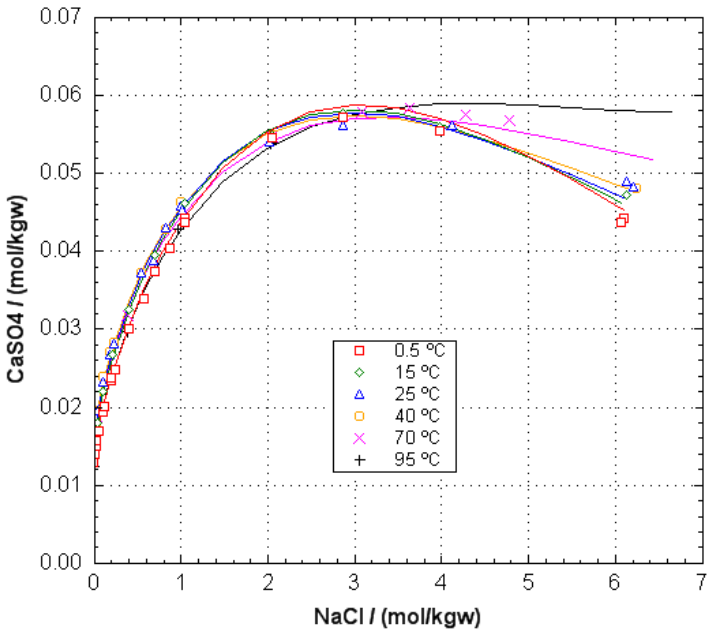

Figure A10. Solubility of gypsum ($CaSO_4:2H_2O$) in NaCl solutions. Data points from Marshall and Slusher, 1966. File gyps_NaCl.phr

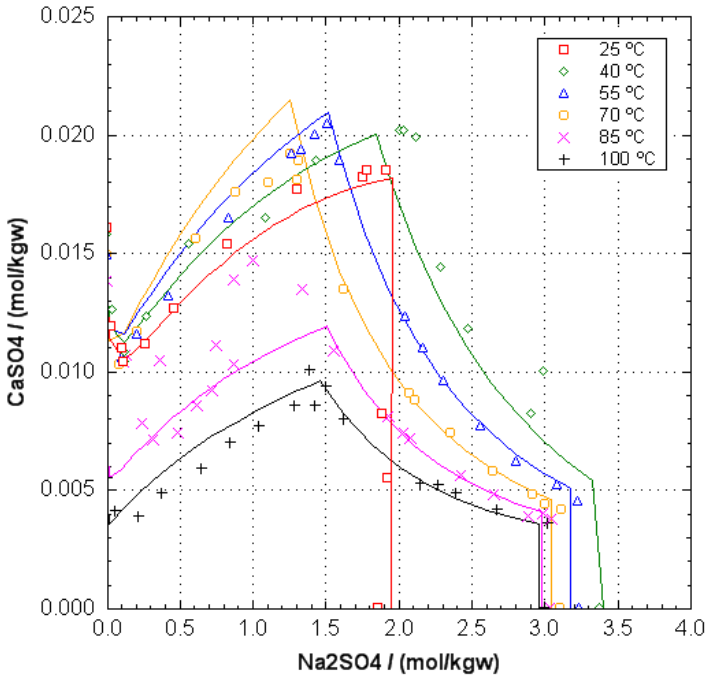

Figure A11. Solubility of gypsum ($CaSO_4 \cdot 2H_2O$) in Na_2SO_4 solutions. Data points from Block and Waters, 1968. File gyps_Na2SO4.phr. The concentration decrease of $CaSO_4$ at Na_2SO_4 concentrations above 1 M is due to mirabilite precipitation (25ºC), or glauberite and thenardite precipitation at higher temperatures. At 85 and 100ºC, and possibly at 70ºC, gypsum transforms into anhydrite.

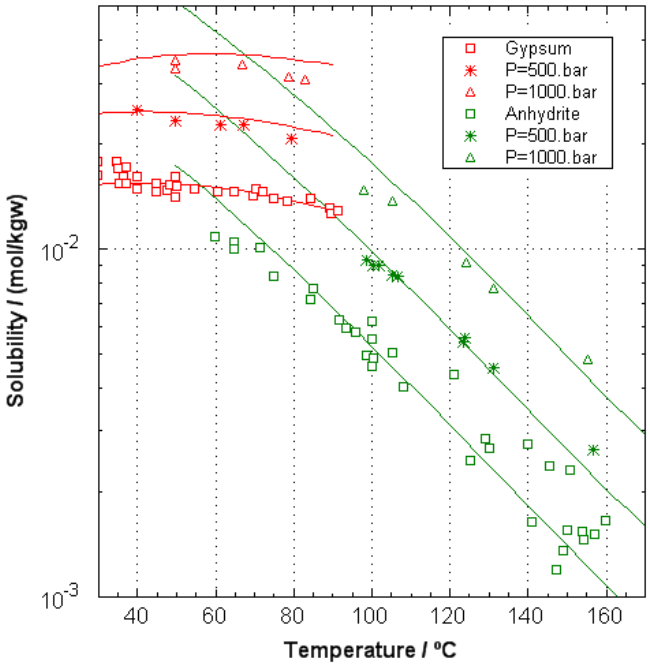

Figure A12. Solubility of gypsum ($CaSO_4 \cdot 2H_2O$) and anhydrite ($CaSO_4$) as a function of temperature and pressure. Data points from Blount and Dickson, 1973. File gypsum_P.phr.

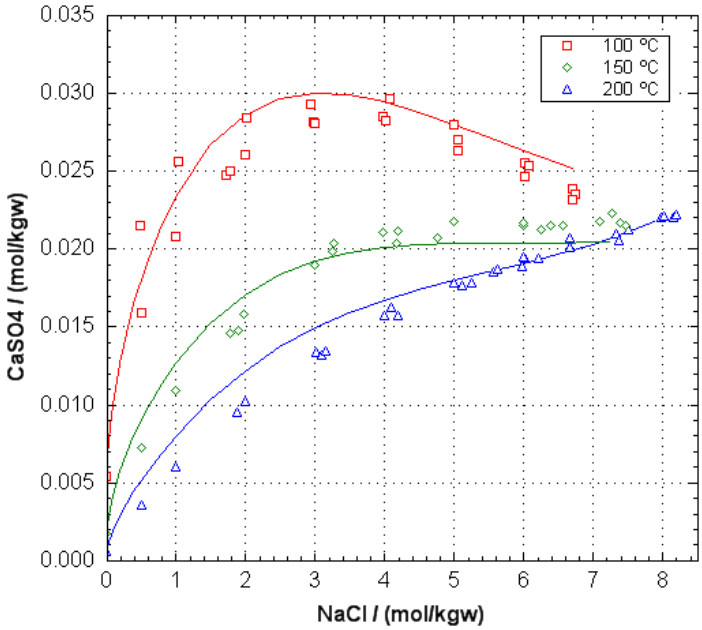

Figure A13. Solubility of anhydrite ($CaSO_4$) in NaCl solutions. Data points from Block and Waters, 1968; Blount and Dickson, 1969; Freyer and Voigt, 2004. File anhy_NaCl.phr.

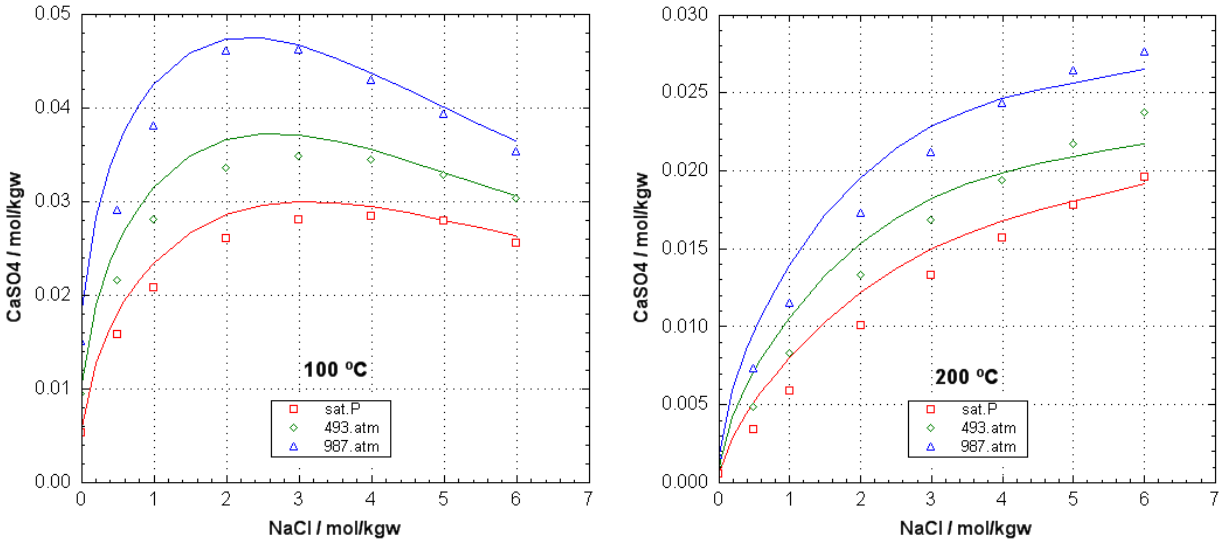

Figure A14. Solubility of anhydrite ($CaSO_4$) in NaCl solutions as a function of pressure at 100ºC and 200ºC. Data points from the summary table in Blount and Dickson, 1969. File anhy_P_NaCl.phr.

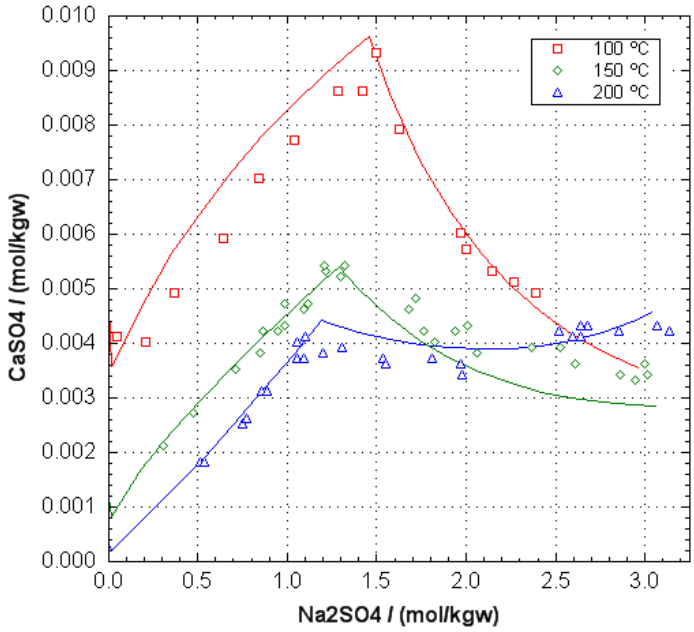

Figure A15. Solubility of anhydrite ($CaSO_4$) in Na_2SO_4 solutions. Data points from Freyer and Voigt, 2004. The decrease of the $CaSO_4$ concentration at Na_2SO_4 concentrations above 1 M is due to glauberite precipitation. File anhy_Na2SO4.phr.

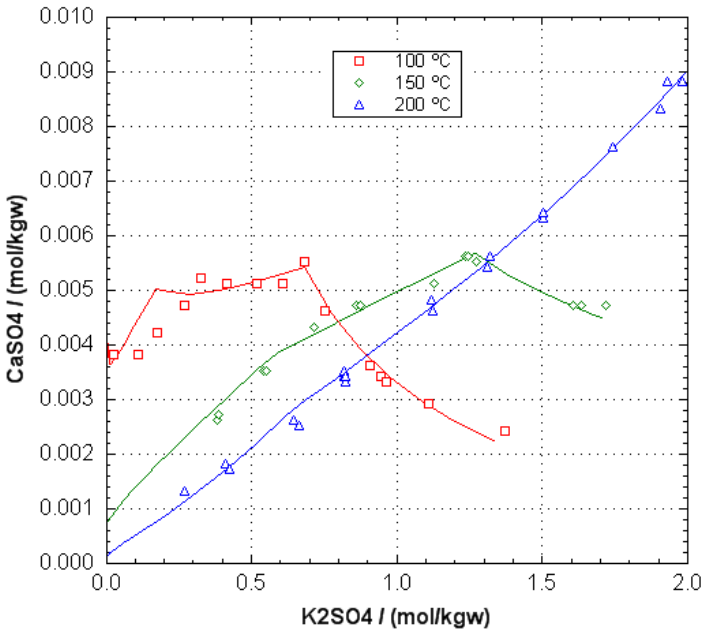

Figure A16. Solubility of anhydrite ($CaSO_4$) in K_2SO_4 solutions. Data points from Freyer and Voigt, 2004. The breaks in the concentration lines result from precipitation of Goergeyite ($K_2Ca_5(SO_4)_6H_2O$) and, at 100 and 150ºC, Syngenite ($K_2Ca(SO4)_2{:}H_2O$). File anhy_K2SO4.phr.

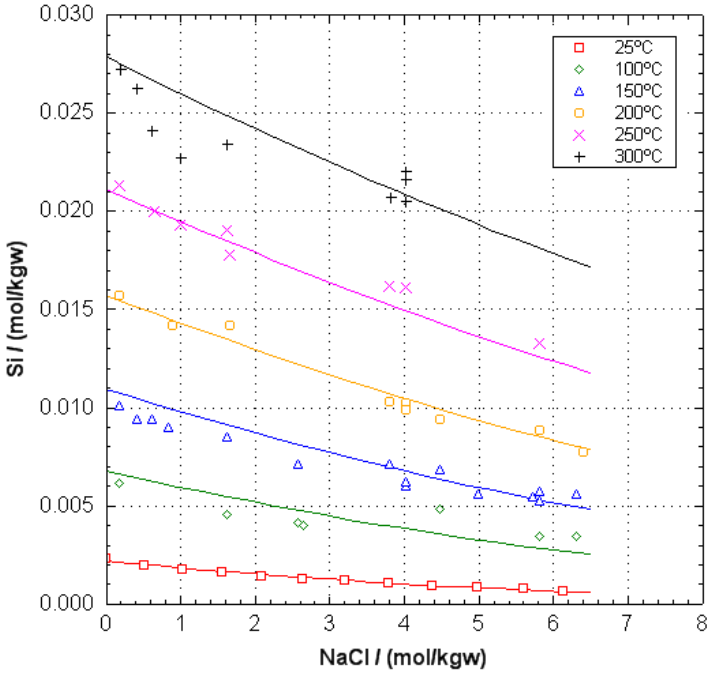

Figure A17. Solubility of amorphous silica (SiO_2(a)) in NaCl solutions. Data points from Marshall and Warakomski, 1980, and Chen and Marshall, 1982. File SiO2_NaCl.phr.

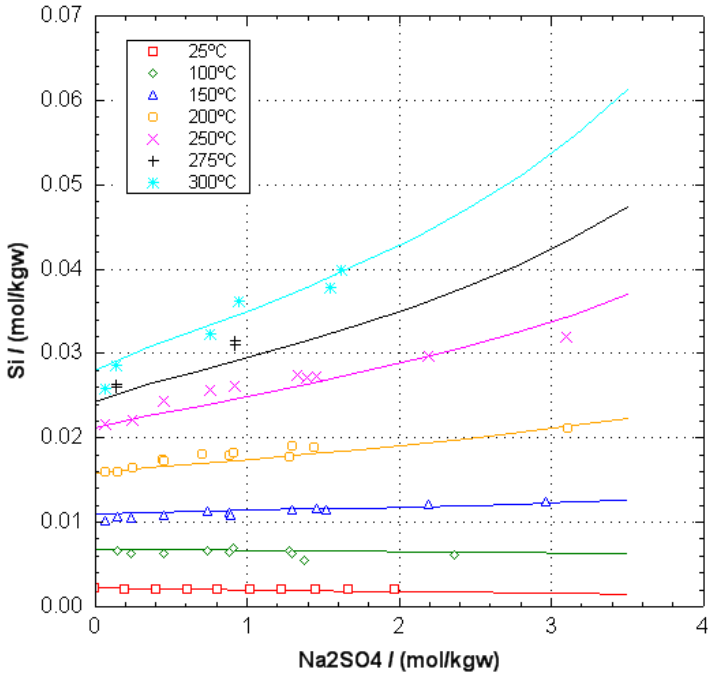

Figure A18. Solubility of amorphous silica (SiO_2(a)) in Na_2SO_4 solutions. Data points from Marshall and Warakomski, 1980, and Chen and Marshall, 1982. File SiO2_Na2SO4.phr.

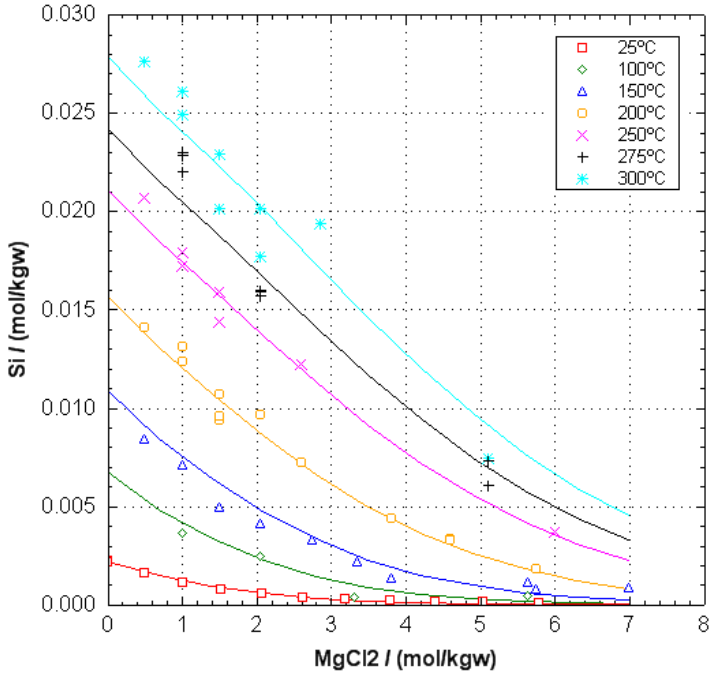

Figure A19. Solubility of amorphous silica (SiO_2(a)) in $MgCl_2$ solutions. Data points from Marshall and Warakomski, 1980, and Chen and Marshall, 1982. File SiO2_ MgCl2.phr.

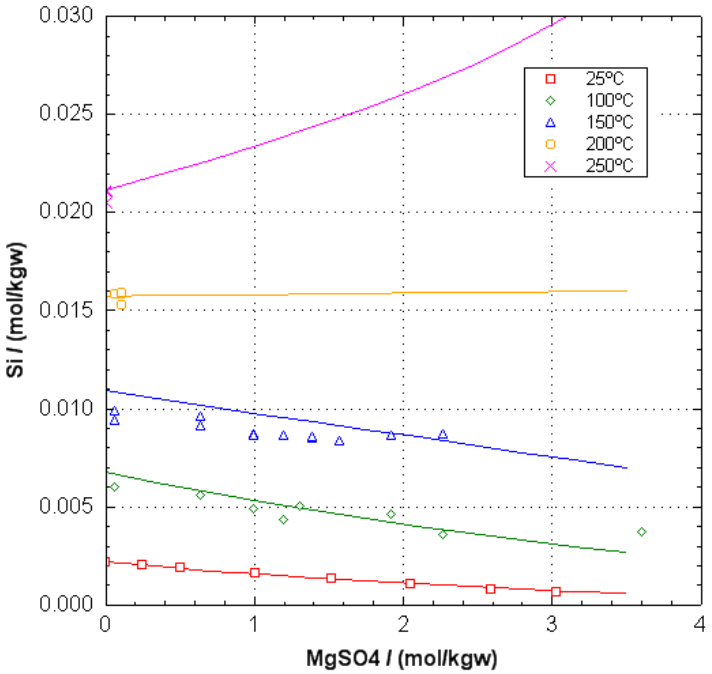

Figure A20. Solubility of amorphous silica (SiO_2(a)) in $MgSO_4$ solutions. Data points from Marshall and Warakomski, 1980, and Chen and Marshall, 1982. File SiO2_MgSO4.phr.

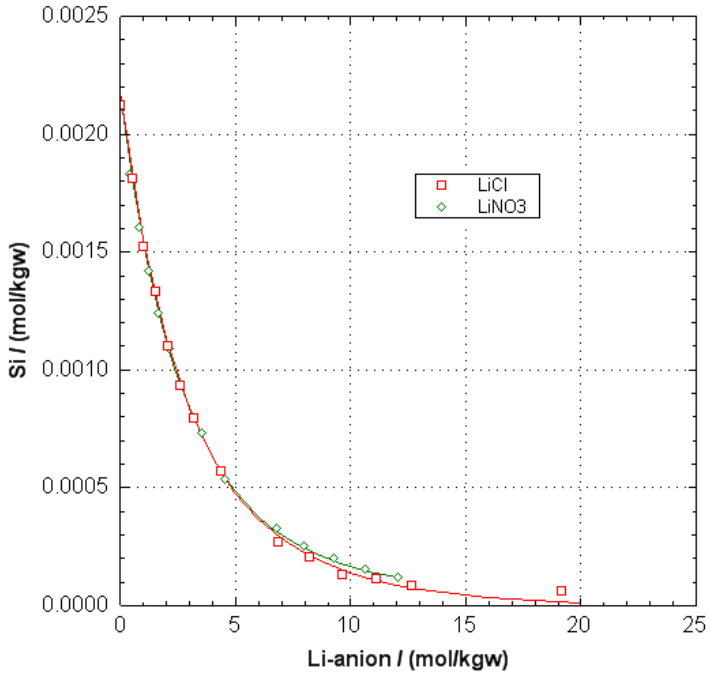

Figure A21. Solubility of amorphous silica (SiO_2(a)) in LiCl and $LiNO_3$ solutions at 25ºC. Data points from Marshall and Warakomski, 1980. File SiO2_Li.phr.

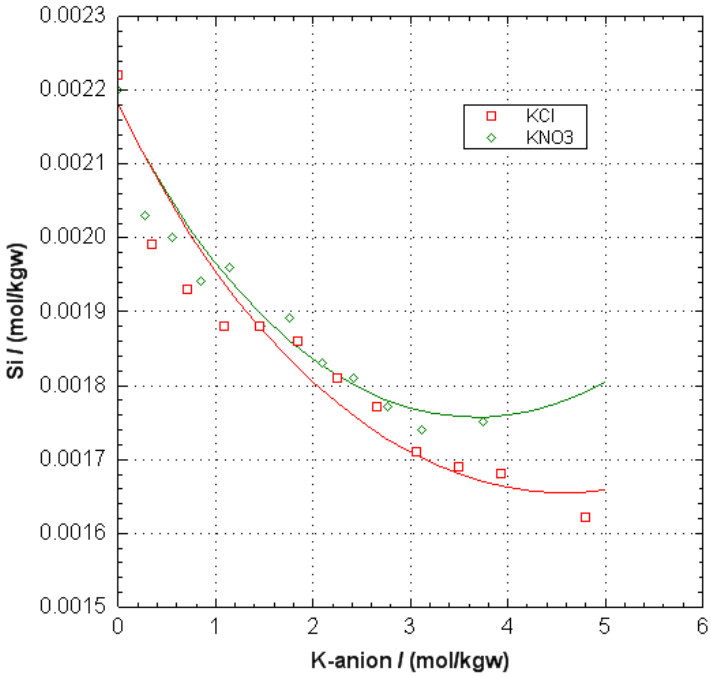

Figure A22. Solubility of amorphous silica (SiO_2(a)) in KCl and KNO_3 solutions at 25ºC. Data points from Marshall and Warakomski, 1980. File SiO2_K.phr.

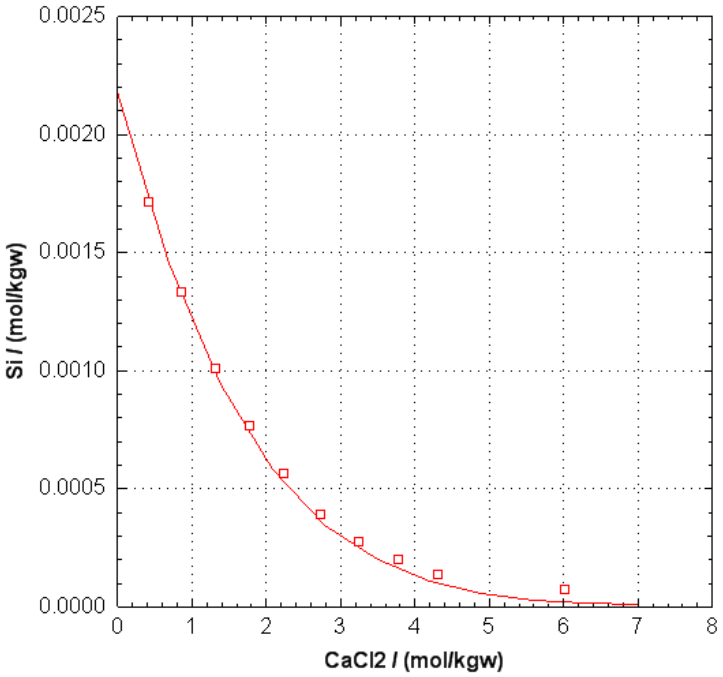

Figure A23. Solubility of amorphous silica (SiO_2(a)) in $CaCl_2$ solutions at 25ºC. Data points from Marshall and Warakomski, 1980. File SiO2_CaCl2.phr.

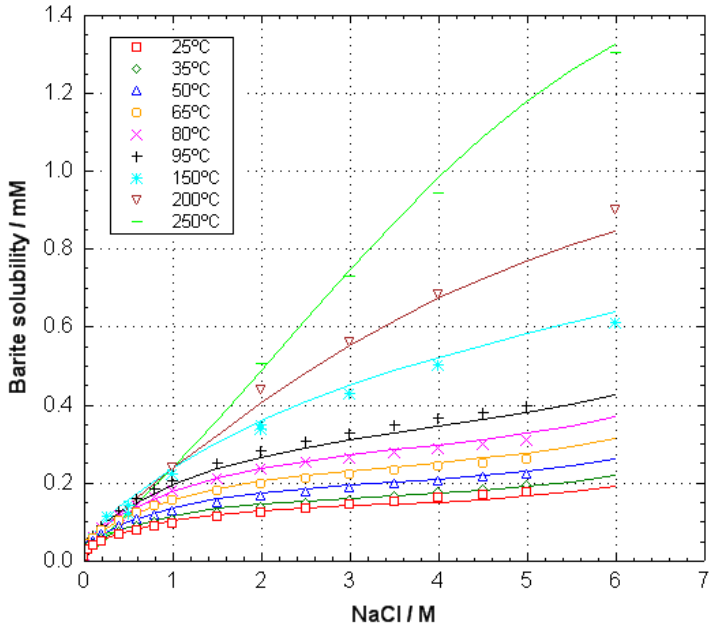

Figure A24. Solubility of barite ($BaSO_4$) in NaCl solutions. Data points < 95ºC from Templeton, 1960, > 100ºC from Uchameyshvili et al., 1966, and the summary table in Blount, 1977. File Barite_NaCl.phr.

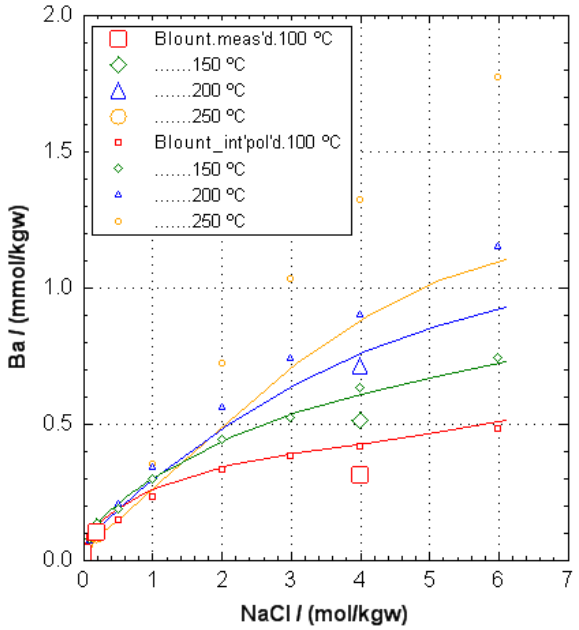

Figure A25. Solubility of barite ($BaSO_4$) in NaCl solutions at 500 bar. Measured (large symbols) and interpolated (small symbols) data from Blount, 1977. File Barite_500.phr.

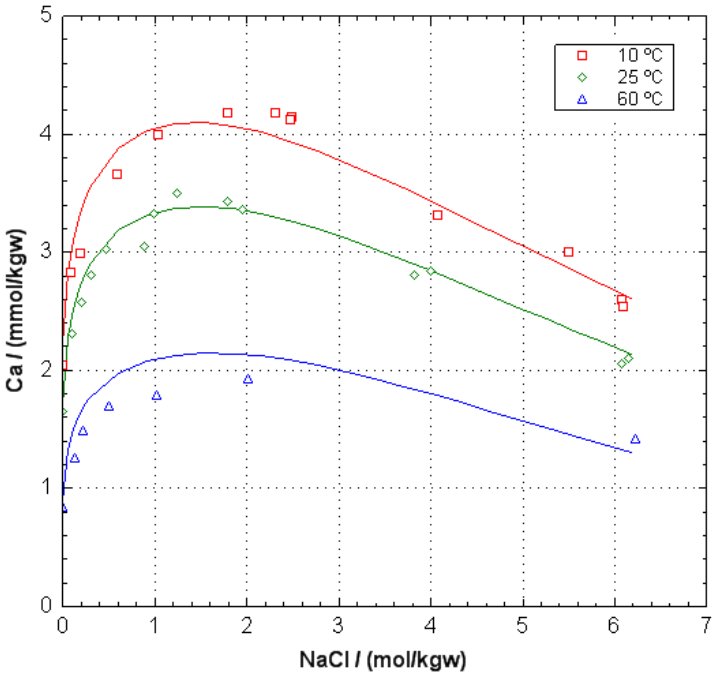

Figure A26. Solubility of calcite ($CaCO_3$) in NaCl solutions at about 0.01 atm CO_2 pressure. Measured data from Wolf et al., 1989. File cc_Wolf.phr.

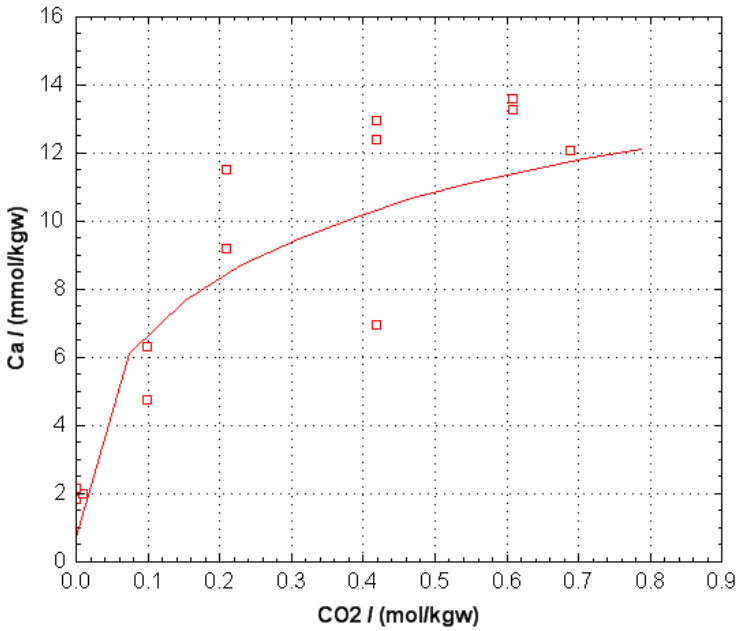

Figure A27. Solubility of calcite ($CaCO_3$) at 200 °C, 580 atm pressure in 3 M NaCl as a function of the CO_2 concentration. Measured data from Malinin and Kanukov, 1971. File cc_Malin.phr.

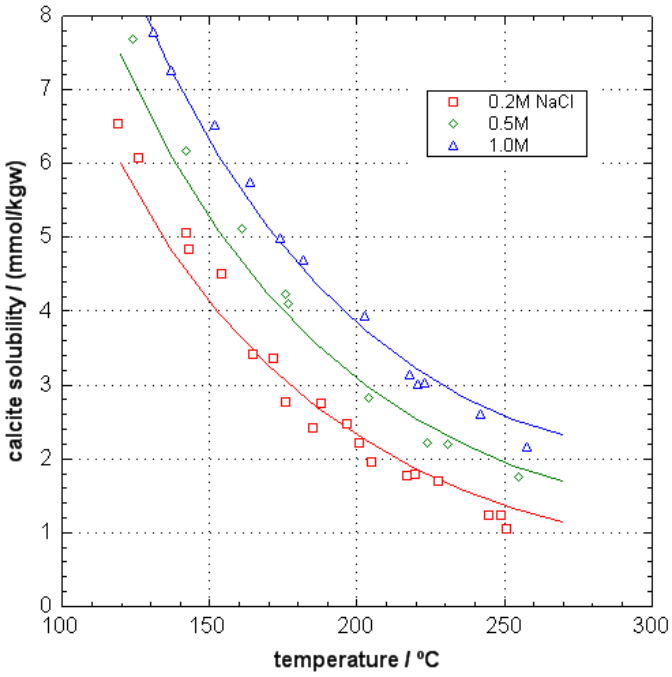

Figure A28. Solubility of calcite ($CaCO_3$) in NaCl solutions at 12 bar CO_2 pressure. Measured data from Ellis, 1963. File cc_Ellis.phr.

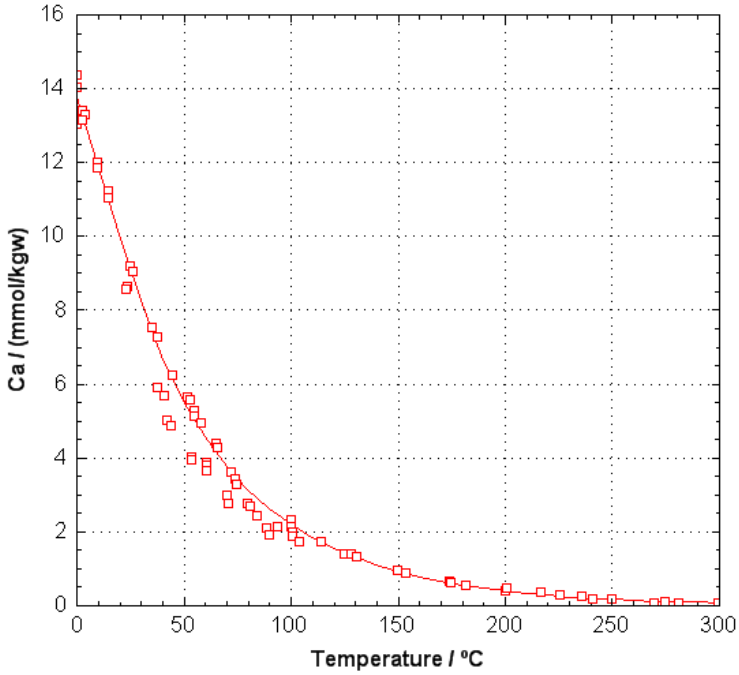

Figure A29. Solubility of calcite ($CaCO_3$) as a function of temperature at 1 bar CO_2 pressure. Measured data from Miller, 1952; Ellis, 1959; Plummer and Busenberg, 1982. File cc_1barCO2.phr.

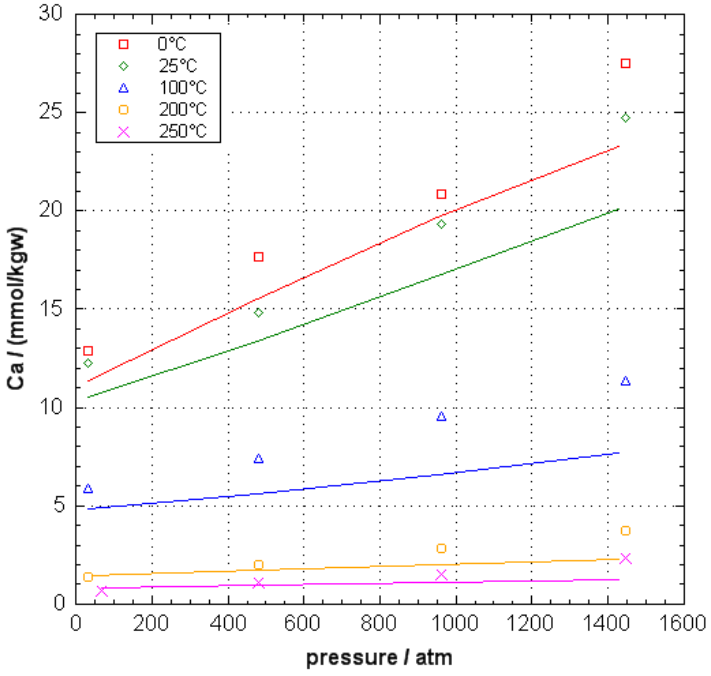

Figure A30. Solubility of calcite ($CaCO_3$) in 0.1 M NaCl as a function of temperature and pressure at 1 bar CO_2 pressure. Measured data from Shi et al., 2013. File cc_Shi.phr. Solubilities at 4 M NaCl and in a brine are also calculated when the file is run.

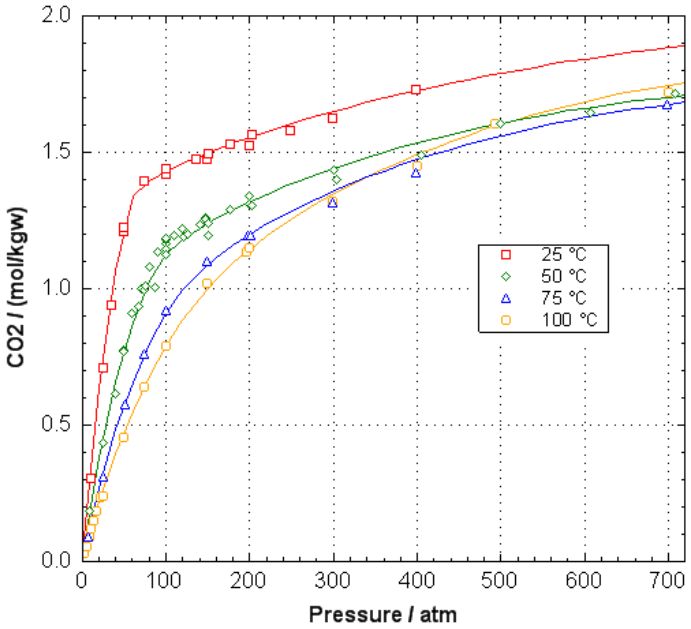

Figure A31. Solubility of CO_2 gas in water. Measured data from Wiebe and Gaddy, 1939, 1940; King et al., 1992; Takenouchi and Kennedy, 1964. File CO2_conc_PR_IS.phr.

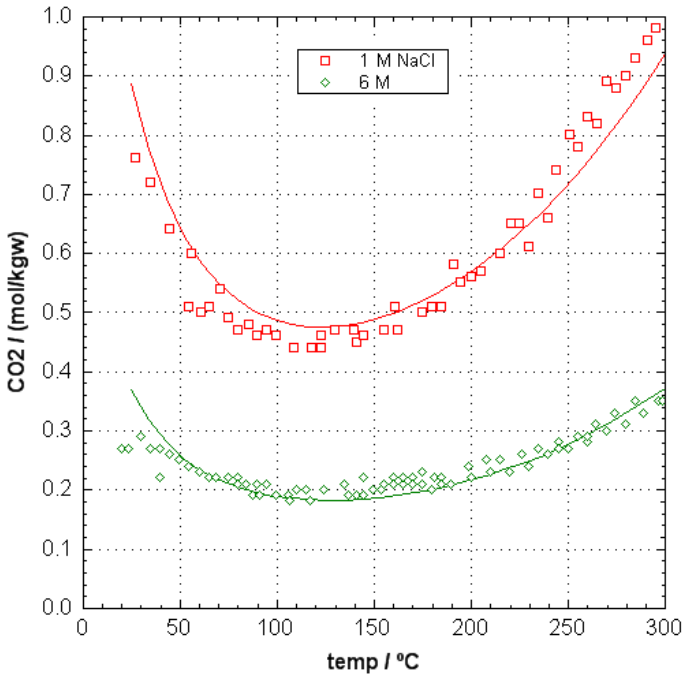

Figure A32. Solubility of CO_2 gas in 1 and 6 M NaCl solutions at about 40 atm CO_2. Measured data from Drummond, 1981. File Drummond.phr.

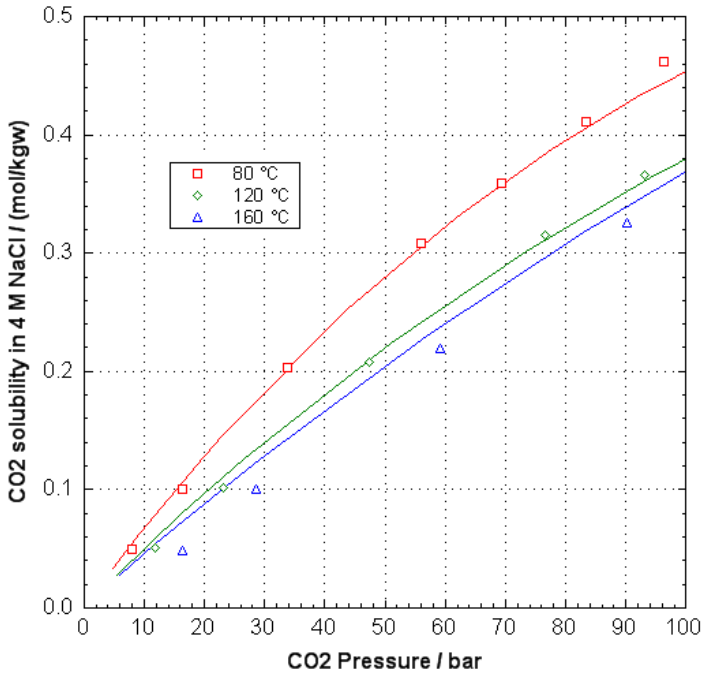

Figure A33. Solubility of CO_2 gas in 4 M NaCl solution. Measured data from Rumpf et al. 1994. File CO2_4M_NaCl.phr.

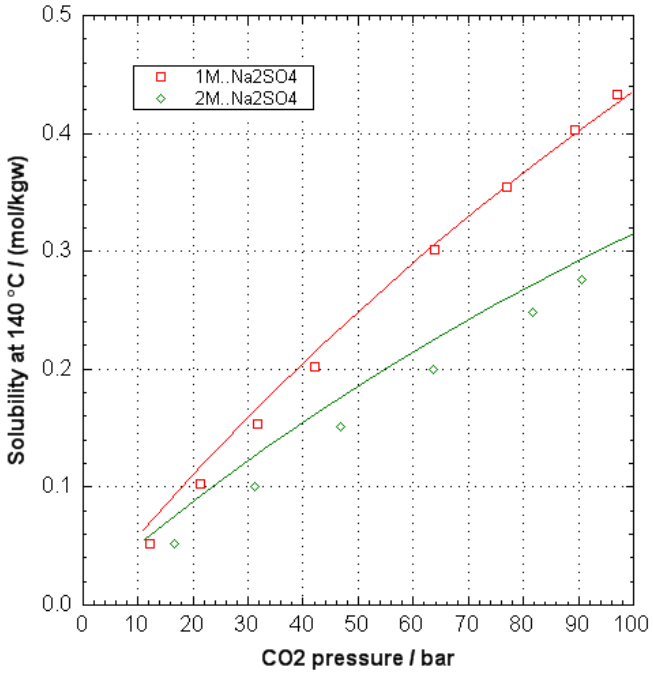

Figure A34. Solubility of CO_2 gas in Na_2SO_4 solutions at 140ºC. Measured data from Rumpf and Maurer, 1993. File P_CO2_Na2SO4.phr.

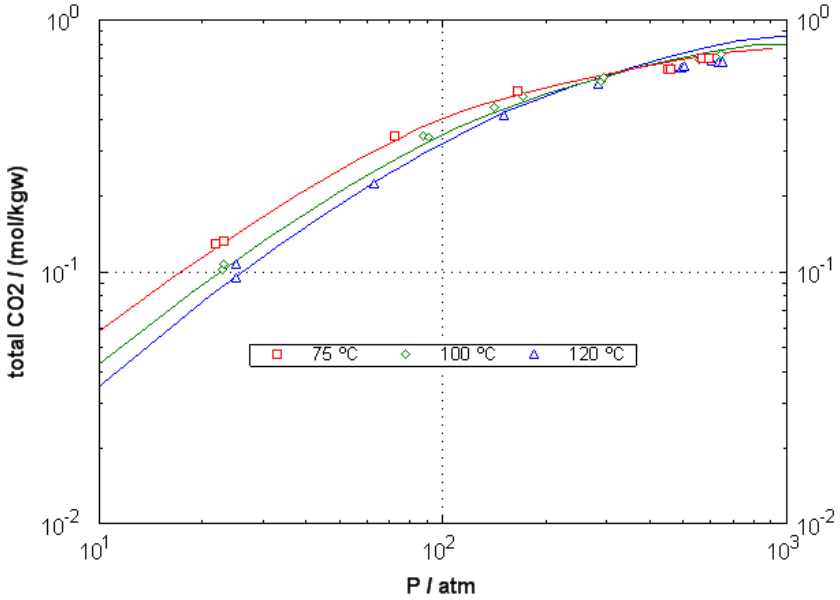

Figure A35. Solubility of CO_2 gas in 2.3 M $CaCl_2$ solution. Data from Springer et al., 2012. File CO2_CaCl2.phr.

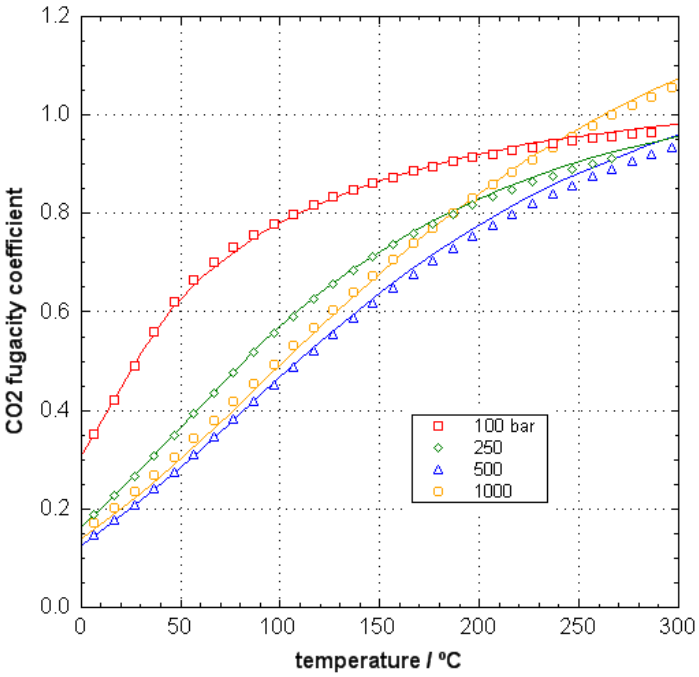

Figure A36. CO_2 fugacity coefficient as a function of temperature for CO_2 gas pressures from 100 - 1000 bar. Data from Angus et al., 1976. File phi_Angus_bar.phr.